Environmental Science & Technology

pubs.acs.org/est

Article

Isoprene–Chlorine Oxidation in the Presence of NO_x and Implications for Urban Atmospheric Chemistry

Dongyu S. Wang,*[,§] Catherine G. Masoud,[§] Mrinali Modi, and Lea Hildebrandt Ruiz*

Cite This: *Environ. Sci. Technol.* 2022, 56, 9251−9264

Read Online

ACCESS | Metrics & More | Article Recommendations | Supporting Information

ABSTRACT: Fine particulate matter ($PM_{2.5}$) is a key indicator of urban air quality. Secondary organic aerosol (SOA) contributes substantially to the $PM_{2.5}$ concentration. Discrepancies between modeling and field measurements of SOA indicate missing sources and formation mechanisms. Recent studies report elevated concentrations of reactive chlorine species in inland and urban regions, which increase the oxidative capacity of the atmosphere and serve as sources for SOA and particulate chlorides. Chlorine-initiated oxidation of isoprene, the most abundant nonmethane hydrocarbon, is known to produce SOA under pristine conditions, but the effects of anthropogenic influences in the form of nitrogen oxides (NO_x) remain unexplored. Here, we investigate chlorine–isoprene reactions under low- and high-NO_x conditions inside an environmental chamber. Organic chlorides including $C_5H_{11}ClO_3$, $C_5H_9ClO_3$, and $C_5H_9ClO_4$ are observed as major gas- and particle-phase products. Modeling and experimental results show that the secondary OH−isoprene chemistry is significantly enhanced under high-NO_x conditions, accounting for up to 40% of all isoprene oxidized and leading to the suppression of organic chloride formation. Chlorine-initiated oxidation of isoprene could serve as a source for multifunctional (chlorinated) organic oxidation products and SOA in both pristine and anthropogenically influenced environments.

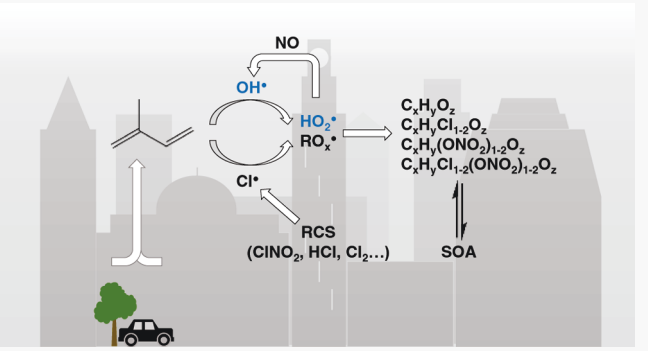

KEYWORDS: *secondary organic aerosol (SOA), chlorine chemistry, isoprene chemistry, anthropogenic−biogenic interactions, reactive chlorine compounds, organochlorides*

INTRODUCTION

Air pollution causes millions of premature deaths each year globally.[1] In particular, exposure to fine suspended particulate matter (PM with a diameter of 2.5 μm or smaller), or aerosol, is shown to be a leading cause of increased morbidity and mortality[1−4] and is expected to worsen for urban populations.[5,6] Aerosol can be primary (i.e., directly emitted) or secondary (e.g., produced from atmospheric chemical processes). Ample evidence shows that secondary organic aerosol (SOA) can contribute substantially to total fine aerosol mass,[7] but the exact contribution by SOA remains highly uncertain. Numerous studies have reported the underestimation of SOA by air quality models,[5,8−10] necessitating a better understanding of SOA sources and formation processes.

In addition to oxidation chemistry driven by ozone (O_3), hydroxyl radicals (OH), and nitrate radicals (NO_3), chlorine radical (Cl) chemistry has been shown to substantially contribute to the atmospheric degradation of anthropogenic emissions,[11,12] inorganic aerosol formation,[13] and secondary organic aerosol formation (SOA).[12] These impacts have been the strongest during wintertime in polluted urban environments,[12,14−19] likely due to increased combustion activities, increased biomass burning, and lowered boundary layer heights contributing to increased concentrations. Under typical ambient conditions, Cl concentrations are thought to range from 10^2 to 10^5 molecules cm^{-3}, one or several orders of magnitude lower than concentrations of the OH radical,[20−22] 10^6 molecules cm^{-3}. However, Cl sources tend to be spatiotemporally localized, with maximum concentrations reaching ~10^6 molecules cm^{-3}.[23−25] Elevated levels of reactive chlorine species, such as molecular chlorine (Cl_2), hydrochloric acid (HCl), hypochlorous acid (HOCl), and nitryl chloride ($ClNO_2$), have been observed in the ambient atmosphere,[11,13,17,23−34] with $ClNO_2$ concentration reaching as high as 8 ppbv.[31] $ClNO_2$ is produced heterogeneously via the reactive uptake of dinitrogen pentaoxide involving chloride (Cl^-)-containing particles.[32,33] $ClNO_2$ accumulates at night and rapidly photolyzes in the early morning to produce Cl radicals and nitrogen dioxide (NO_2). $ClNO_2$ and Cl

Received: October 20, 2021
Revised: May 23, 2022
Accepted: May 24, 2022
Published: June 14, 2022

https://doi.org/10.1021/acs.est.1c07048
Environ. Sci. Technol. 2022, 56, 9251−9264

productions are heavily influenced by anthropogenic activities and are known to occur in coastal, industrial, and urban regions.[13,24,26,32,34] Modeling studies show that Cl chemistry can dominate the early morning organic peroxy radical production and increase the oxidative capacity by enhancing the production of hydrogen oxide radicals (HO_x) and ozone.[17,27−29,34] Non-negligible levels of $ClNO_2$ and molecular chlorine (Cl_2) have also been reported well into midday.[11,23−25,30] Furthermore, the use of chlorine-containing products such as cleaning solutions could be a significant source of indoor air pollution (e.g., hundreds of ppbv of reactive chlorine species and ∼10^7 molecules cm^{-3} of Cl radicals) and a health threat to building occupants.[35−40] All told, the impact of Cl chemistry on air quality and health may be more pervasive than previously thought.[17−19,23,26,28,41]

Despite recent advances, significant knowledge gaps remain regarding the source, oxidation chemistry, reaction products, and the fate of reactive chlorine species.[12,42] Cl-initiated SOA production from biogenic (e.g., α-pinene, isoprene, *d*-limonene) and anthropogenic (e.g., alkanes, toluene, polycyclic aromatic hydrocarbons) volatile organic compound (VOC) precursors have been reported in environmental chamber studies.[40,43−50] Cl oxidation products have been observed in the gas and particle phases under ambient conditions,[23] notably isomers of 1-chloro-3-methyl-3-butene-2-one (C_5H_7ClO), i.e., "CMBO", a well-known tracer for Cl−isoprene chemistry.[23,51−54] Isoprene (2-methyl-1,3-butadiene, C_5H_8) is the most abundantly emitted biogenic nonmethane hydrocarbon with an annual emission rate of roughly 500 Tg.[55] Globally, vegetation accounts for over 90% of isoprene emission,[56] but anthropogenic isoprene sources such as traffic emissions could become important in urban environments, especially during winter months when biogenic emissions are low.[57−59] Isoprene chemistry has far-reaching implications for air quality,[60] climate,[61] and health.[62] Under most ambient conditions, OH radicals are the dominant sink for isoprene.[42] OH−isoprene oxidation initiates via OH addition to the less substituted terminal carbons (i.e., ∼70% to C_1 and ∼30% to C_4) followed by a reversible O_2 addition.[42] The resulting RO_2 radicals can undergo termination reactions with hydroperoxyl radicals (HO_2) to form isoprene hydroxyhydroperoxide (ISOPOOH, $C_5H_{10}O_3$), undergo isomerization reactions, or react with nitrogen oxide (NO). ISOPOOH can further react with OH radicals to form either isoprene epoxydiol (IEPOX, $C_5H_{10}O_3$), which can undergo acid-catalyzed reactive uptake reactions,[63−68] or a dihydroxy hydroperoxy peroxy radical ($C_5H_{11}O_6$), which can produce highly functionalized, low-volatility reaction products.[69−73] Due to its fast reaction rate coefficient with OH radicals (∼1×10^{-10} cm^3 $molecules^{-1}$ at 298 K), isoprene could act as a OH scavenger and suppress SOA formation from other VOCs, such as monoterpenes and aromatics.[74−76]

The reaction rate coefficient of Cl with isoprene is 4.1×10^{-10} cm^3 $molecules^{-1}$ at 298 K, roughly 4 times higher than that of OH with isoprene.[42,77,78] Cl−isoprene reaction occurs via Cl addition (85%) and H-abstraction (∼15%).[23−25] Quantum chemical calculation suggests that Cl addition favors terminal carbons, C_1 (36.9%) and C_4 (45.7%) present on the double bonds, with H-abstraction favoring tertiary hydrogen.[79] Theoretical calculations also suggest that the RO_2 radicals produced from Cl−C_4 addition could undergo rapid intramolecular H-shift (0.2 s^{-1}), allowing for further O_2 addition via the autoxidation mechanism,[80] which is rapid enough to compete with reactions with NO (1.4 s^{-1}) and termination with HO_2 radicals (0.02 s^{-1}) under typical ambient conditions.[42,79] Given the high abundance of isoprene and the localized, elevated reactive chlorine concentrations, Cl−isoprene oxidation could be a significant source of SOA and highly oxygenated organic molecules (HOMs).[79] Our previous study shows that the Cl-initiated oxidation of isoprene under dry, low-NO_x conditions produces multifunctional chlorinated and nonchlorinated oxidation products based on gas-phase chemical ionization mass spectrometry (CIMS) measurements.[45] Formation of particulate organic chlorides was expected based on the gas-phase composition but could not be directly verified at the time using aerosol chemical speciation monitor (ACSM) measurements alone. Similarly, little is known about Cl−isoprene chemistry under high-NO_x conditions beyond the composition of first-generation gas-phase products.[51,77,81]

In this study, we investigate the chlorine-initiated oxidation of isoprene under low- and high-NO_x conditions in the presence of neutral or acidified seed particles through a series of environmental chamber experiments. We show the formation of multifunctional gas-phase products and, for the first time, SOA production from Cl−isoprene reactions under high-NO_x conditions. Using the Filter Inlet for Gasses and AEROsols (FIGAERO)-CIMS, we were able to confirm the presence of organic chloride in Cl−isoprene SOA produced under both low- and high-NO_x conditions. Our experimental and modeling results show that the presence of NO_x significantly enhances secondary OH chemistry during Cl−isoprene oxidation, resulting in the formation of products typically attributed to OH−isoprene chemistry.

MATERIALS AND METHODS

Experiments were performed in a temperature-controlled 10 m^3 Teflon environmental chamber operated in batch mode at room temperature.[82] Molecular Cl_2 (Airgas, 100.3 ppm in N_2) was injected into the chamber as the Cl precursor. For high-NO_x experiments, NO (Airgas, 97.7 ppm in N_2) was injected into the chamber. Isoprene injection was performed by flowing dry, zero air supplied by a clean air generator (Aadco, 737R) over microliters of isoprene liquid (Acros Organics, 98%) placed inside a glass sampling tube (Kimble-Chase, 250 mL). Seed particles were generated using either an aqueous 0.05 M ammonium sulfate ($(NH_4)_2SO_4$) or an aqueous 0.005 M sulfuric acid (H_2SO_4) solution with an aerosol generation system (Brechtel, AGS model 9200) to explore the effect of extreme pH. The seed particles generated from $(NH_4)_2SO_4$ were assumed to be near-neutral, while the seed particles generated from H_2SO_4 were assumed to be highly acidic. Precursor concentrations were allowed to stabilize before switching on the ultraviolet (UV-A) lights to photolyze Cl_2 into Cl to initiate Cl−isoprene oxidation reactions. The UV intensity was similar to solar irradiation[83] at a zenith angle of 53° based on the measured NO_2 photolysis rate at 0.37 min^{-1}. The UV lights were switched off after 60 min. The O_3 and NO_x concentrations were measured using a photometric ozone analyzer (Teledyne, 400E) and a chemiluminescence NO_x monitor (Teledyne, 200E), respectively. Between experiments, the chamber was cleaned by first flushing zero air at >100 L min^{-1} (LPM) for >12 h; high concentrations of O_3 (>1 ppm) were then injected into the chamber, and UV lights were turned on for >6 h; finally, the chamber was flushed with zero air for >12 h. For humid experiments, clean air was passed

https://doi.org/10.1021/acs.est.1c07048
Environ. Sci. Technol. 2022, 56, 9251−9264

through heated DI water and injected into the chamber, which was held at an elevated temperature. At the end of the humidification period and prior to the injection of precursors, the chamber temperature was restored back to room temperature to increase the RH.

Experimental conditions are summarized in Table 1. Experiments 1−3 were conducted under high-NO_x conditions, and exps. 4−6 were conducted under low-NO_x conditions to investigate the effects of NO_x on gas- and particle-phase oxidation product compositions. Experiments 4 and 5 were conducted under dry (<5% RH) and humid (>60% RH) conditions with identical precursor gas concentrations to examine the effect of RH. Sulfuric acid seed particles were used in exps. 3 and 6 to examine the effect of low aerosol pH. Ammonium sulfate seed particles were used for the rest of the experiments listed in Table 1. Cl and OH radical concentrations during the photooxidation period were estimated using the SAPRC model with a condensed carbon-bond mechanism augmented with additional isoprene and Cl−isoprene reaction pathways (see the Supporting Information (SI)).[84] In particular, the fraction of isoprene oxidized by OH radicals, $f_{\mathrm{Isop+OH}}$, was estimated using the model

$$f_{\mathrm{Isop+OH}} = \frac{M_{\mathrm{Isop+OH}}}{M_{\mathrm{Isop+OH}} + M_{\mathrm{Isop+Cl}}} \quad (1)$$

where $M_{\mathrm{Isop+OH}}$ and $M_{\mathrm{Isop+Cl}}$ are the cumulative amount of isoprene oxidized by OH and Cl radicals by the end of the 60 min photooxidation period, respectively. The (secondary) OH concentration may be experimentally estimated by monitoring the decay of isoprene in experiments with and without benzene added as a OH scavenger. This was not performed here due to the lack of sensitivity of iodide chemical ionization mass spectrometry (I^--CIMS) toward nonoxidized compounds such as isoprene.

Bulk aerosol chemical composition was characterized by a quadrupole aerosol chemical speciation monitor (ACSM, Aerodyne Inc.) operated at a 200 ms amu^{-1} scan speed with a roughly 1 min resolution. Data were analyzed in Igor 8 (Wavemetrics Inc.) using the ACSM Local package (Aerodyne Research Inc.). A default relative ionization efficiency (RIE) value of 1.4 was used for particulate organics. Calibration with dried, size-selected (300 nm) ammonium chloride (NH_4Cl) particles yielded an RIE value of 1.44 for chloride, which is similar to the default value of 1.3,[85] which was ultimately used here. Note that NH_4Cl is nonrefractory and has higher RIE values than semirefractory species, e.g., sodium chloride.[86] If organic chlorides are not nonrefractory, using RIE values calibrated using NH_4Cl may underestimate chloride concentration. Particulate chloride concentration was estimated using the m/z 36 ions (HCl^+), which responds promptly to changes in chloride concentration, unlike the m/z 35 ions (Cl^+).[45,86] The response factor of NO_3 and the RIE of NH_4 were determined using dried, size-selected (300 nm) ammonium nitrate (NH_4NO_3) particles generated by nebulizing a 0.005 M aqueous NH_4NO_3 solution. The RIE of SO_4 was determined using dried, size-selected (300 nm) $(NH_4)_2SO_4$ particles generated by nebulizing a 0.005 M aqueous $(NH_4)_2SO_4$ solution following standard procedures.[87] The total SOA concentration is calculated as the sum of organics, nitrate, and chloride concentrations as measured by the ACSM, assuming a collection efficiency of 0.5 for the ammonium sulfate seeds.[88]

Table 1. Summary of Experimental Conditions and Results[a]

exp.	Cl_2	VOC	NO	RH	seed	phase	MW	comp.	SOA	seed	Chl/Org	NO_3/Org	f_{91}	f_{82}
1	100	98	80	55	$(NH_4)_2SO_4$	gas	153	$C_{4,6}H_{7,9}Cl_{0,3}N_{0,7}O_{4,4}$						
						particle	169	$C_{6,2}H_{10,2}Cl_{0,2}N_{0,3}O_{4,7}$	10	16	0.61×10^{-2}	7.70×10^{-2}	0.74×10^{-2}	1.20×10^{-2}
2	100	244	82	45	$(NH_4)_2SO_4$	gas	152	$C_{4,6}H_{7,9}Cl_{0,4}N_{0,6}O_{4,2}$						
						particle	166	$C_{5,8}H_{10,2}Cl_{0,3}N_{0,3}O_{4,5}$	22	26	0.98×10^{-2}	8.25×10^{-2}	0.46×10^{-2}	1.02×10^{-2}
3	200	489	160	75	H_2SO_4	gas	148	$C_{4,1}H_{6,8}Cl_{0,6}N_{0,5}O_{4,1}$						
						particle	158	$C_{5,2}H_{8,8}Cl_{0,4}N_{0,3}O_{4,2}$	76	77	5.20×10^{-2}	10.30×10^{-2}	0.60×10^{-2}	1.72×10^{-2}
4	200	489	0	4	$(NH_4)_2SO_4$	gas	158	$C_{5,2}H_{8,6}Cl_{0,8}N_{0,1}O_{3,5}$						
						particle	189	$C_{6,4}H_{9,8}Cl_{0,7}N_{0,1}O_{4,7}$	91	63	4.76×10^{-2}	4.61×10^{-2}	0.64×10^{-2}	0.59×10^{-2}
5	200	489	0	61	$(NH_4)_2SO_4$	gas	150	$C_{4,8}H_{7,9}Cl_{1,1}N_{0,0}O_{2,9}$						
						particle	185	$C_{6,5}H_{10,2}Cl_{0,8}N_{0,0}O_{4,4}$	62	39	3.72×10^{-2}	4.03×10^{-2}	0.55×10^{-2}	0.51×10^{-2}
6	200	489	0	58	H_2SO_4	gas	134	$C_{4,3}H_{7,1}Cl_{0,9}N_{0,0}O_{2,8}$						
						particle	148	$C_{5,2}H_{8,2}Cl_{0,5}N_{0,1}O_{3,7}$	97	78	7.94×10^{-2}	4.32×10^{-2}	0.47×10^{-2}	1.10×10^{-2}

[a]Cl_2, VOC (isoprene), and NO are the initial concentrations in ppbv. RH is in %. Molecular weight (MW) is in g mol^{-1}. Ratios derived using ACSM measurements are dimensionless, where Chl/Org is the ratio of particulate chloride (estimated using the HCl^+ signal at m/z 36) to organics, NO_3/Org is the ratio of particulate NO_3 to organics, and f_{91} and f_{82} are the fractional contributions to total organic concentration by ions observed at m/z 91 and 82, respectively. The average MW and elemental composition (comp.) are determined using (FIGAERO-)CIMS measurements. SOA concentration in $\mu g\ m^{-3}$ is calculated as the sum of the organics, nitrate, and chloride concentrations measured by the ACSM using eq S3 for wall loss correction. Seed particle concentration in $\mu g\ m^{-3}$ is calculated as the sum of SO_4 and NH_4 measured by the ACSM at the start of the photooxidation period. The ACSM collection efficiency is assumed to be 0.5. The pH of sulfate seed particles is estimated using the extended aerosol inorganic model,[97,98] as described in further detail in the SI.

https://doi.org/10.1021/acs.est.1c07048
Environ. Sci. Technol. 2022, 56, 9251−9264

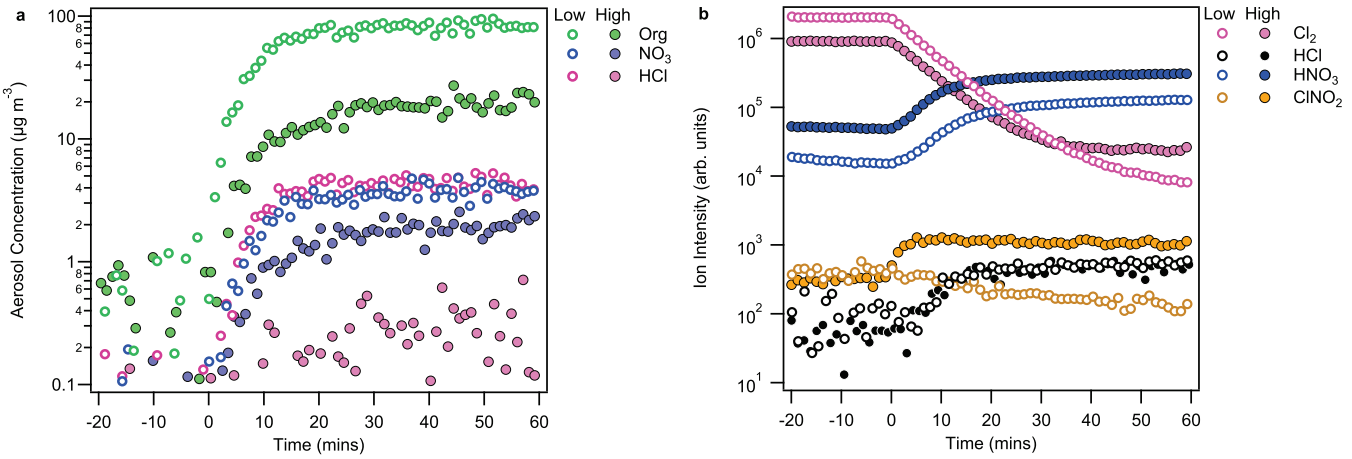

Figure 1. Comparison of select (a) bulk particle-phase species observed by the ACSM and (b) inorganic gas-phase species observed by the FIGAERO-CIMS under high-NO_x (exp. 2, in solid markers) and low-NO_x (exp. 4, in hollow markers) oxidation conditions. UV lights were turned on at minute 0 to initiate photooxidation reactions and turned off at minute 60.

Wall loss was corrected using eq S3 based on the sulfate inorganic seed ratio method.[89]

Gas-phase composition was characterized by iodide chemical ionization mass spectrometry (I^--CIMS) with a high-resolution time-of-flight mass analyzer (HTOF, Tofwerk AG and Aerodyne Research Inc.). A methyl iodide permeation source was flushed with a 2 LPM dry nitrogen flow, which was then passed through a polonium-210 radiation source before entering the ion−molecule reaction region of the HTOF operated at 100 mbar. Although some deprotonated ions (i.e., $[M - H]^-$) were observed, we only consider I^- adducts, i.e., $[M + I]^-$ in our analysis. Particle-phase composition was characterized by a Filter Inlet for Gasses and AEROsols (FIGAERO, Aerodyne Research Inc.),[90] which was operated in the gas sampling mode for at least the first 60 min from the start of photooxidation. Afterward, the FIGAERO alternated between the gas sampling/aerosol collection and aerosol desorption mode. In the aerosol collection mode, particles are collected onto a polytetrafluoroethylene (PTFE) membrane filter at 3 LPM for 15 min. The desorption cycle lasts for 45 min: 20 min for temperature ramp-up from 25 to ∼200 °C, 15 min for soaking at ∼200 °C, and 10 min for cool-down. For experiments 1 and 2 (see Table 1), where the SOA loadings were relatively low, the collection time was extended to 60 min with no changes made to the temperature ramp-up procedure. CIMS and FIGAERO data were analyzed using Tofware 3.2 in Igor 8. Oxidation products containing five or fewer carbon atoms are considered as monomers, while those containing six or more carbon atoms are considered dimers/oligomers. It should be noted that thermal decomposition is a known issue for FIGAERO-CIMS and other thermal volatilization-based detection techniques, where the breakdown of larger accretion products could produce fragments resembling monomers.[90−93] Multimodal thermograms are telltale signs of thermal decomposition. Product ion intensities are normalized by the reagent ion signal, I^-. To estimate the relative aerosol composition, we assume a uniform response factor for all $[M + I]^-$ ions and weigh their ion intensities by the molecular weight of the neutral analyte. I^--CIMS is known to favor acidic and moderately to highly oxygenated compounds.[94−96] Intercomparison of the I^--FIGAERO-CIMS with a high-resolution aerosol mass spectrometer (AMS), which functions similarly to the ACSM for bulk aerosol quantification, has shown that the two instruments agree within ±50% for OH−isoprene SOA if a uniform sensitivity (i.e., that of formic acid) is applied to the sum of I^--FIGAERO-CIMS ions.[73]

RESULTS AND DISCUSSION

SOA production from Cl−isoprene oxidation was observed under low- and high-NO_x conditions, as shown in Figure 1a. The bulk aerosol composition as measured by the ACSM was predominately comprised of organics. The relative contribution by particulate NO_3, presumably from organic nitrates, was enhanced under high-NO_x conditions compared to that of low-NO_x conditions, as shown in Table 1. The initial Cl_2 concentrations used are much higher than ambient levels, which was necessary to drive oxidation chemistry and produce sufficient SOA mass within the short time scale of environmental chamber experiments (minutes to hours) relative to ambient oxidation time scales (days to weeks). One result of using the high precursor concentrations may be the increased importance of RO_2 + RO_2 reaction pathways in these experiments compared to the ambient.

Under low-NO_x conditions, the increase in RH appears to suppress the SOA formation, as shown in Table 1 for exp. 4 (91 $\mu g\ m^{-3}$ of SOA produced at <5% RH) and exp. 5 (62 $\mu g\ m^{-3}$ of SOA produced at ∼61% RH). Suppression of SOA formation by increasing RH has also been reported for OH−isoprene oxidation in the presence of NO_x.[99] Increased vapor wall loss under humid conditions[100] and reduced particle-phase reactions due to the lower initial seed particle concentrations may also contribute to the lower SOA production in exp. 5 compared to that in exp. 4. The addition of NO_x also appears to suppress SOA formation, as shown in Table 1 and Figure S2 when comparing exp. 3 (76 $\mu g\ m^{-3}$ of SOA produced under high NO_x) and exp. 6 (97 $\mu g\ m^{-3}$ of SOA produced under low NO_x). Because the ACSM utilizes a fragmentation table to estimate NO_3 mass based on the m/z 30 and 46 ions, the production of organic ions such as CH_2O^+ (m/z 30) and $CH_2O_2^+$ (m/z 46) may contribute to the apparent observation of organic nitrate under low-NO_x conditions. Furthermore, the chamber was not NO_x-free during low-NO_x experiments, as evident in the production of HNO_3 observed by I^--FIGAERO-CIMS (Figure 1b). The presence of background NO_x, e.g., from the production of nitrous acid over Teflon surfaces,[84] is a known issue for

https://doi.org/10.1021/acs.est.1c07048
Environ. Sci. Technol. 2022, 56, 9251−9264

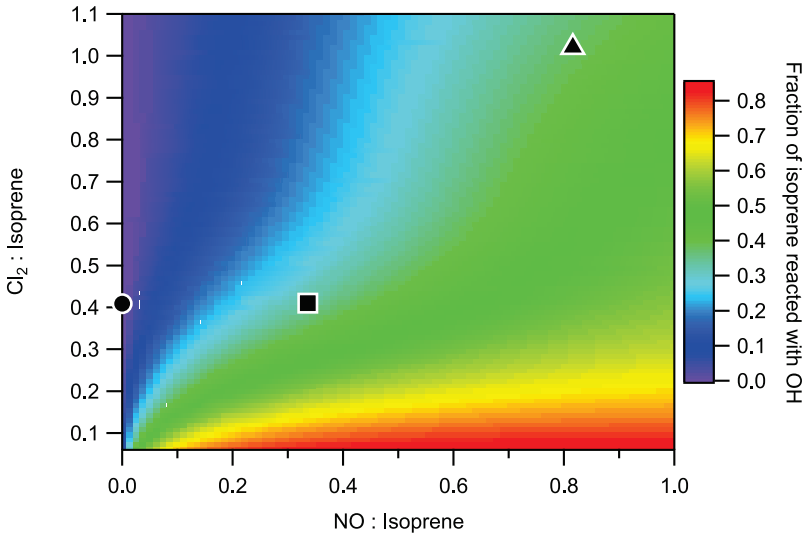

Figure 2. Amount of isoprene oxidized by the OH radical as a fraction of the total amount of isoprene oxidized, i.e., by both OH and Cl radicals, as estimated using eq 1 based on chamber model results. The respective ratios of Cl_2 and NO concentrations relative to that of isoprene prior to the photooxidation period are shown on the *y*- and *x*-axes. The Cl_2-to-isoprene and NO-to-isoprene ratios used in the experiments are indicated by a triangle for exp. 1, a square for exps. 2 and 3, and a circle for exps. 4–6.

environmental chambers. The particulate organic chloride concentration, qualitatively represented here by the ACSM measurement of HCl^+ at m/z 36,[45] was suppressed under high-NO_x conditions (exps. 1 and 2) compared to low-NO_x conditions (exps. 4 and 5), as shown in the ratio of chloride-to-organics (Chl/Org) in Table 1. The Chl/Org ratios as measured by the ACSM for bulk aerosol composition were higher when acidified seed particles were used, which was not accompanied by an increase in the organic chloride content, as measured by the FIGAERO-CIMS. This suggests that the additional chloride could come from the uptake of inorganic chlorides, such as HCl by the H_2SO_4 seed particles (exps. 3 and 6), which behave more liquid-like than $(NH_4)_2SO_4$ particles.

Modeling of the Cl–isoprene oxidation chemistry under high-NO_x conditions, shown in Figure 2, suggests that up to 40% of all isoprene consumed can be attributed to the secondary OH radical chemistry. In contrast, the secondary OH chemistry is negligible under the low-NO_x condition, accounting for less than 0.1% of the isoprene oxidized at all times. The reduction in the relative contribution by particulate chloride under high-NO_x conditions may, in part, be explained by the competition between OH– and Cl–isoprene chemistries. The fractional contribution of the organic signal at m/z 82 (presumably $C_5H_6O^+$) to the total organic signal measured by the ACSM, f_{82}, was higher for SOA produced under high-NO_x or acidic conditions, as shown in Table 1, which points to the increased contribution from IEPOX SOA as the result of the secondary isoprene–OH chemistry.[101] The fractional contribution to total organic ions at m/z 91, f_{91}, presumably by $C_7H_7^+$ fragments from particle-phase ISOPOOH accretion products[72] was not systematically different between high- and low-NO_x experiments. In addition to the secondary OH chemistry, the enhanced production of other reactive species such as O_3 and $ClNO_2$ was observed under high-NO_x conditions, as shown in Figures 1b and S2. Consistent with previous modeling studies,[17,27−29,34] results here show that the isoprene–chlorine chemistry in the presence of NO_x could enhance the oxidative capacity of the atmosphere.

Gas-Phase Composition. Oxidation products with the highest ion intensities observed under low- and high-NO_x conditions are shown in Figure 3a,b, respectively. Reactions of Cl_2 or HOCl with unsaturated VOCs such as monoterpenes, furans, and isoprene have been reported previously,[40,102,103] although it only becomes significant for isoprene when its initial concentration is very high (>10 ppm).[40] HOCl concentration was negligible, and no increase in gas-phase oxidation products was observed before the UV lights were turned on, suggesting that dark reactions between Cl_2 and isoprene were negligible under these conditions. Under low-NO_x conditions, C_5 organic chlorides ($C_xH_yCl_zO_w$, abbreviated as CHClO) such as $C_5H_8Cl_2O_3$, $C_5H_9ClO_2$, $C_5H_9ClO_3$, $C_5H_{10}Cl_2O_2$, and $C_5H_{11}ClO_3$ dominate. The presence of dichlorinated compounds is indicative of multigenerational oxidation chemistry driven by Cl addition to the unsaturated carbon(s) present on initial oxidation products. Nonchlorinated organics ($C_xH_yO_z$, abbreviated as CHO) also account for a substantial portion of the gas-phase oxidation products even under low-NO_x (i.e., low OH) conditions (Figures 3a and S4a,e), notably $C_5H_6O_3$, possibly a HO_2 termination product of RO_2 radical derived from H-abstraction of C_5H_6O, one of the proposed oxidation products from the H-abstraction of isoprene.[81] In addition, one of the most abundant gas-phase oxidation products, $C_5H_{10}O_3$ has a molecular formula that is consistent with ISOPOOH, IEPOX (OH oxidation product of ISOPOOH), or C_5-alkene triol;[63,64,71,91,104,105] the use of chromatographic separation or tandem mass spectrometry is required to differentiate these compounds. Its time series trend (rapid increase followed by decay) represents that of a reactive initial oxidation product. The scarcity of OH radicals produced from Cl–isoprene oxidation under low-NO_x conditions and the prominence of $C_5H_{10}O_3$ suggest that it may be an isomer of ISOPOOH that is produced from non-OH–isoprene pathways. It is also possible that the I^--CIMS is more selective toward $C_5H_{10}O_3$ or that some key OH radical generation pathways involving Cl–isoprene chemistry are not accounted

https://doi.org/10.1021/acs.est.1c07048
Environ. Sci. Technol. 2022, 56, 9251−9264

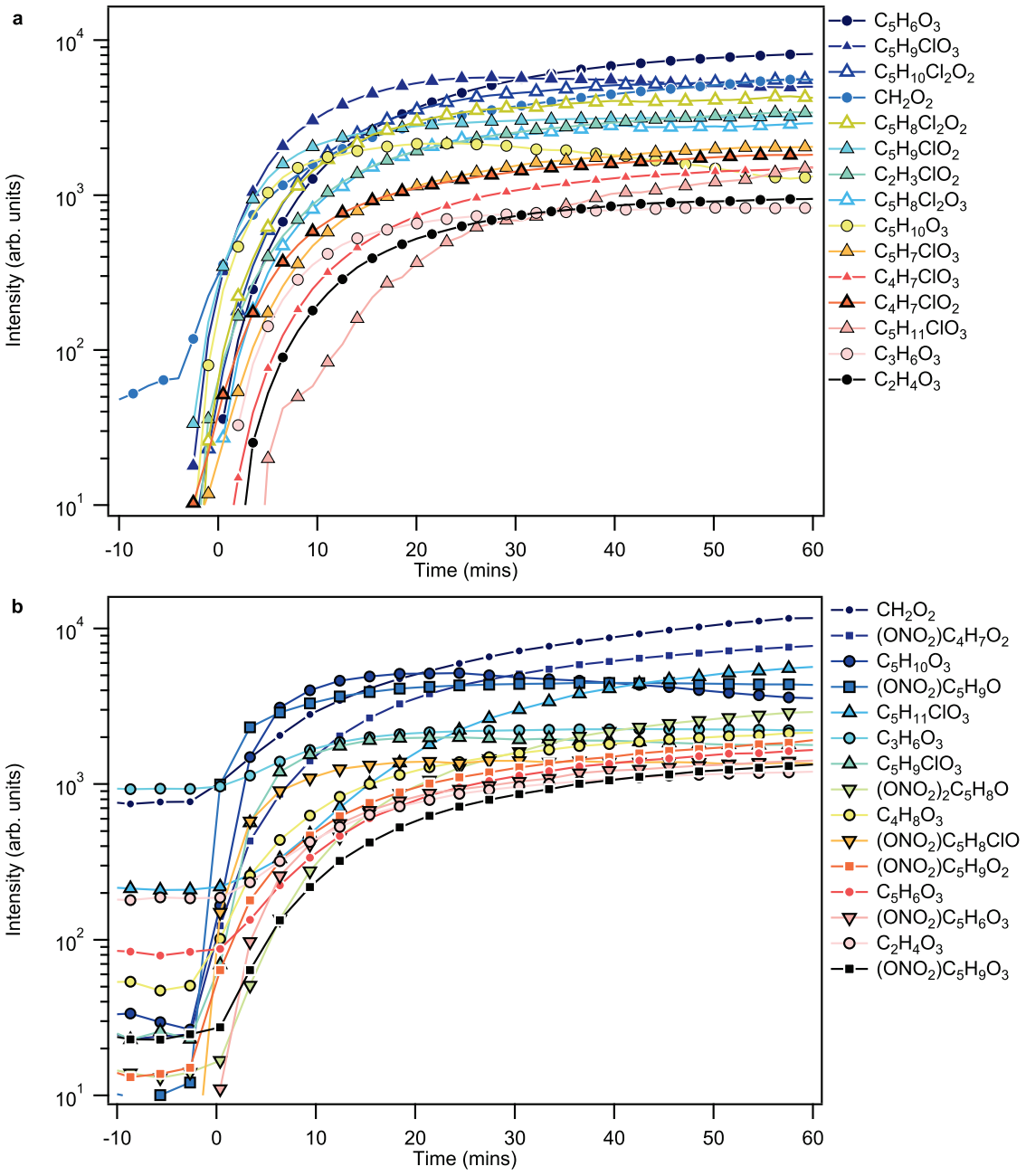

Figure 3. (a) Time series of the most intense ions observed under low-NO_x conditions from exp. 4. (b) Time series of the most intense ions observed under high-NO_x conditions from exp. 2. The ion intensities are ranked based on their average over the photooxidation period, with the corresponding neutral analyte formula displayed in the legend in descending order.

for in the condensed mechanism used in the model. In addition to species resembling OH−isoprene oxidation products, isomer(s) of $C_3H_7ClO_3$, $C_3H_5ClO_3$, $C_4H_7ClO_2$, and $C_5H_7ClO_2$, which have been observed in the atmosphere but were attributed to traffic emission sources,[11] were observed from Cl−isoprene oxidation under low- and high-NO_x conditions (Figures 3 and S4b,f), where $C_4H_7ClO_2$ is one of the dominant gas-phase products under low-NO_x conditions, as shown in Figure 3a. Thus, Cl−isoprene chemistry could contribute to the formation of organic chlorides that would be otherwise attributed to the degradation of anthropogenic VOCs (e.g., C_3 and C_4 precursors).

A quantum chemical calculation study has proposed $C_5H_9ClO_2$ as the HO_2 termination product of Cl−C_1 addition to the RO_2 radical, whereas $C_5H_7ClO_3$ and $C_5H_9ClO_4$ (not shown in Figure 3a, but observed) were proposed to be autoxidation products derived from the Cl−C_4 addition RO_2 radical.[79] Cl−isoprene oxidation products such as C_5H_7ClO, $C_5H_9ClO_2$, and $C_5H_9ClO_3$ were observed by an I^--FIGAERO-CIMS in the gas and particle phases in a polluted, semirural environment.[23] While $C_5H_9ClO_2$ and $C_5H_9ClO_3$ have been observed as two of the most abundant gas-phase oxidation products under both low- and high-NO_x chamber conditions, we did not observe appreciable signals corresponding to C_5H_7ClO using I^--CIMS, i.e., $[C_5H_7ClO + I]^-$, which would occupy the same unit-mass with $[C_5H_{10}O_3 + I]^-$ that dominates the signal at m/z 245. As shown in our previous work on the Cl−isoprene oxidation under low-NO_x conditions,

https://doi.org/10.1021/acs.est.1c07048
Environ. Sci. Technol. 2022, 56, 9251−9264

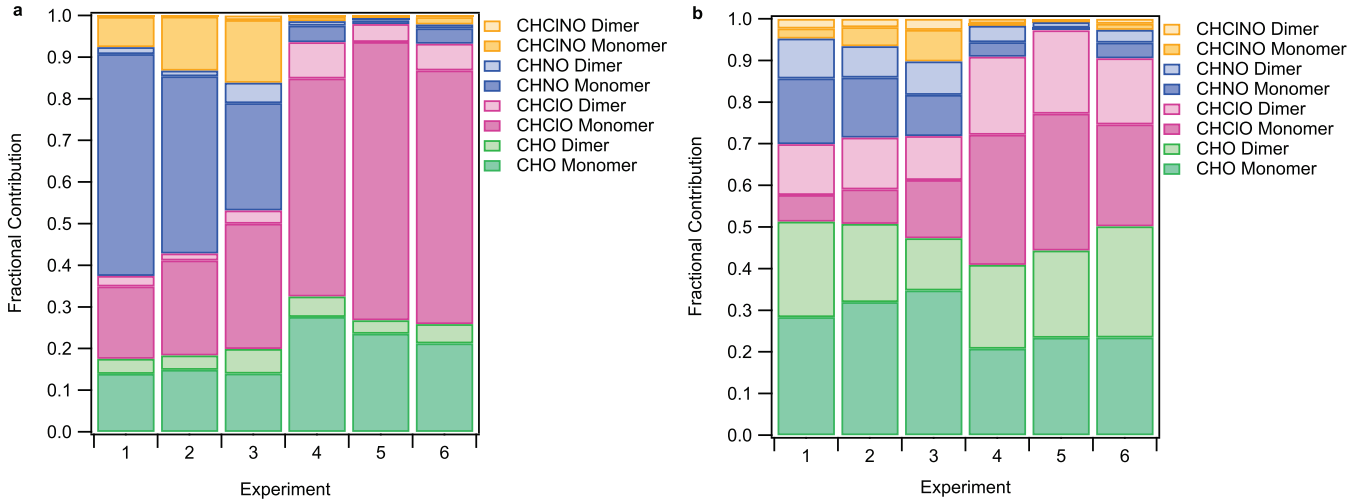

Figure 4. (a) Fractional contribution to the total gas-phase concentration by oxidized organic compounds (CHO), organic chloride (CHClO), organic nitrate (CHNO), and chlorinated organic nitrate (CHClNO). (b) Fractional contribution to the particle-phase concentration by CHO, CHClO, CHNO, and CHClNO. For both panels (a) and (b), ion intensities are weighted by the molecular weight of the neutral analyte to represent the contribution of each group of species to the total concentration on a mass basis. $C_{>5}$ oxidation products are assumed to be dimers. The average gas-phase composition during the 15 min filter collection period and the blank-corrected, average particle-phase composition during the 45 min filter desorption periods are shown in panels (a) and (b), respectively.

ions consistent with CMBO could be observed in the positive ion mode using water-hydronium CIMS and presumably also using proton-transfer-reaction mass spectrometry, as $[C_5H_7ClO + H]^+$.[45] Because CMBO is one of the main expected oxidation products from Cl−isoprene, this suggests that I^--CIMS may not be sensitive toward lowly oxygenated organic chlorides, such as chloroacetic acid ($C_2H_3ClO_2$), whose response factor by I^--CIMS is reportedly 3 times lower than that of formic acid (CH_2O_2).[23] However, the sensitivity difference observed between chloroacetic acid and formic acid may not apply to all chlorinated and nonchlorinated oxidation products because I^--CIMS sensitivity can also vary substantially for different compounds,[106,107] and it was recently shown to be structure-dependent based on isomer-resolved measurements.[108] If a uniform response factor is assumed, CHClO and CHO dominate the gas-phase composition with negligible contribution (<5%) by organic nitrate ($C_xH_yN_zO_u$, abbreviated as CHNO) and organic nitroxychlorides ($C_xH_yCl_zN_uO_v$, abbreviated as CHClNO) under low-NO_x conditions, as shown in Figure 4a.

Under high-NO_x conditions, CHNO dominates the total gas-phase mass concentrations (>50%), whereas the contribution by CHClO (<15%) is greatly suppressed, especially dichlorinated species (Figures 3b and 4a; Table S1c). In molar terms, Figure 3b shows that the most intense oxidation products observed include CH_2O_2 (presumably formic acid), $(ONO_2)C_4H_7O_2$, $C_5H_{10}O_3$ (e.g., isomers of ISOPOOH, IEPOX, or C_5-alkene triol), $(ONO_2)C_5H_9O_2$, and $(ONO_2)C_5H_9O_3$, all of which have been also reported as major gas-phase OH−isoprene oxidation products, which is consistent with the enhanced secondary OH chemistry under high-NO_x conditions. Increase in the CH_2O_2 concentration under high-NO_x condition has also been reported for the OH−isoprene oxidation and was attributed to fragmentation reactions.[71] Under high-NO_x conditions, $ISOPO_2$ + NO competes with $ISOPO_2$ + HO_2 to produce organic nitrate, as well as methyl vinyl ketone (MVK) and methacrolein (MACR), which have been observed from Cl−isoprene oxidation under low-NO_x conditions as well.[42,45,81] Although ions consistent with MVK/MACR ($[C_4H_6O + I]^-$) were not observed by I^--CIMS due to their low oxygen content, ions consistent with its OH + NO_x oxidation products such as $(ONO_2)C_4H_7O_2$, methacrylic acid epoxide (MAE, $C_4H_6O_3$), or hydroxymethyl-methyl-α-lactone (HMML, also $C_4H_6O_3$)[42,109,110] were observed in the gas phase, as shown in Figures 3 and S4. In the presence of O_3 and NO_x, N_2O_5 production and NO_3 radical chemistry may be viable. In addition, the decomposition of methacryloylperoxynitrate (MPAN) produces MAE/HMML and NO_3, acting as another potential source for NO_3 chemistry. Figure S4 shows that MPAN was not among the most abundant products observed, which suggests that its production was minor. It is possible, however, that MPAN is unstable and could decompose when analyzed using I^--CIMS. During the UV irradiation period, ions associated with NO_3 radicals such as $[N_2O_5 + I]^-$ were negligible. The SAPRC model also predicts little contribution of NO_3 radical chemistry to isoprene oxidation during this period (<2% of the total amount consumed). Therefore, the contribution of NO_3−isoprene chemistry to Cl-initiated photooxidation of isoprene under high-NO_x conditions is likely minor.

Compounds with molecular formulae consistent with 2-methylglyceric acid (2MGA, $C_4H_8O_4$), methyltetrol (MT, $C_5H_{12}O_4$), trihydroxyhydroperoxide ($C_5H_{12}O_5$), isomers of methylerythronic acid or methylthreonic acid ($C_5H_{10}O_5$) and hydroxyl dihydroxyperoxy aldehyde ($C_5H_{10}O_6$) were observed as minor high-NO_x Cl−isoprene oxidation products (see Figure S5a). MT and 2MGA are expected products of reactive uptake of IEPOX,[111,112] though recent studies point to potential gas-phase formation mechanisms for these compounds.[113] Compounds such as $C_5H_{12}O_5$, $C_5H_{10}O_5$, $C_5H_{10}O_6$, and $C_5H_{10}O_7$ have been identified as LVOC products of the dihydroxy hydroperoxy peroxy radical, $C_5H_{11}O_6$, from the non-IEPOX pathway of OH−ISOPOOH oxidation.[69,70] The $C_5H_{11}O_6$ radical may also undergo rapid isomerization reactions (k_{iso} > 0.1 s^{-1}), which is competitive against bimolecular reactions under ambient conditions, forming products such as $C_5H_{10}O_6$ (with HO_2) and $C_5H_{10}O_5$ (decomposition).[70]

https://doi.org/10.1021/acs.est.1c07048
Environ. Sci. Technol. 2022, 56, 9251−9264

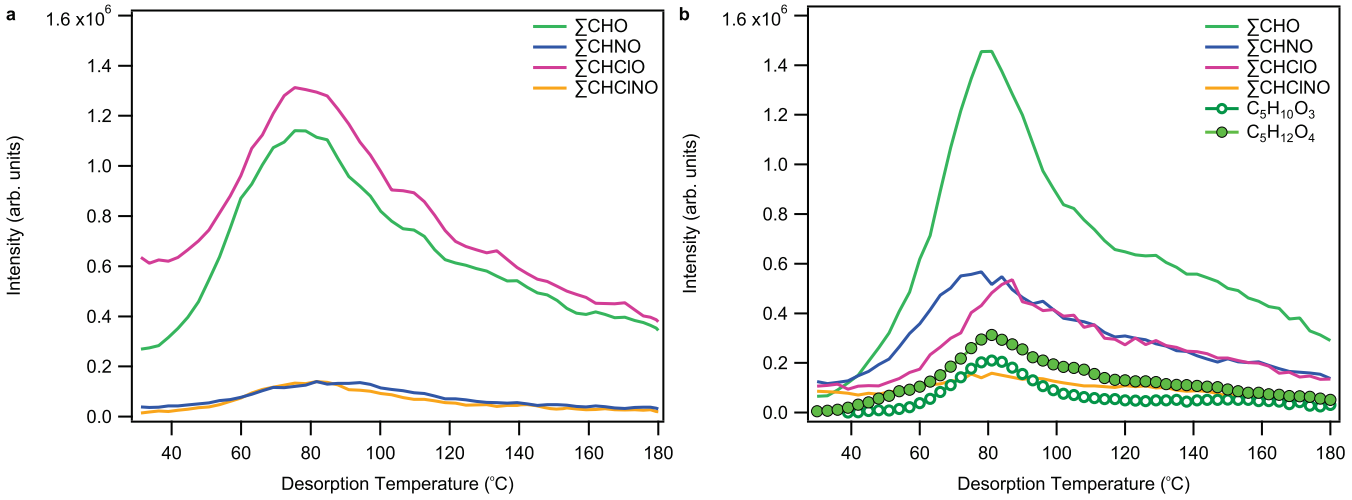

Figure 5. (a) Thermogram of the summed CHO, CHClO, CHNO, and CHClNO compounds observed in the particle phase by I^--FIGAERO-CIMS in exp. 4 under low-NO_x condition and (b) that observed in exp. 2 under high-NO_x condition. $C_5H_{10}O_3$ and $C_5H_{12}O_4$, whose thermograms are shown in panel (b), are included in the total CHO. Ion intensity shown is weighted by molecular weights and therefore corresponds to the mass concentrations.

The HO_2 termination product of $C_5H_{11}O_6$ and one of the most abundant gas-phase oxidation products of OH−ISOPOOH reactions, $C_5H_{12}O_6$, identified as dihydroxy dihydroperoxide ($ISOP(OOH)_2$),[69] were not observed in either gas or particle phase during chlorine-initiated oxidation of isoprene in this study. The HO_2 + RO_2 chemistry may not be competitive against RO_2 + NO and/or RO_2 + RO_2 reactions for $C_5H_{11}O_6$ under the given chamber conditions. $C_5H_{11}O_6$ may have been scavenged by NO under our experimental conditions, leading to the formation of (ONO_2)-$C_5H_{11}O_4$, which was observed (Figure S5a), or $C_5H_{11}O_5$, an alkoxy radical.[70] It is also possible that $C_5H_{10}O_3$ (the precursor for $C_5H_{11}O_6$) reacts with Cl, e.g., via H-abstraction, to form $C_5H_9O_5$ radical, which reacts with NO to form (ONO_2)-$C_5H_9O_3$ or via Cl addition to form $C_5H_{10}ClO_3$, which can then undergo termination reaction with HO_2 to form $C_5H_{11}ClO_3$. Both $(ONO_2)C_5H_9O_3$ and $C_5H_{10}ClO_3$ are among the most abundant CHClO products observed in the gas phase under high-NO_x conditions. Overall, our results show that while secondary OH chemistry may contribute substantially to the initial oxidation of isoprene and product formation (i.e., $C_5H_{10}O_3$) under high-NO_x conditions, Cl and NO chemistries heavily influence the subsequent multigenerational chemistries, resulting in distinct product composition.

Particle-Phase Composition. The bulk SOA composition estimated using I^- adducts detected by FIGAERO is shown in Figure 4b, and the thermograms of CHO, CHClO, CHNO, and CHClNO compounds are shown in Figure 5a,b for a low-NO_x (exp. 4) and a high-NO_x (exp. 2) experiment, respectively. Overall, accretion products ($C_{>5}$ compounds) account for a substantial fraction of the particulate mass under both low- and high-NO_x conditions (>30%; Figure 4b), unlike that for the gas mass concentration, where the contribution of accretion products is minor (<15%), especially under high-NO_x conditions (<10%, Figure 4a). It is worth noting that Lopez-Hilfiker et al. (2016, ES&T) observed more than one local T_{max} value in $C_5H_{10}O_3$ and $C_5H_{12}O_4$ thermograms from their ambient measurement. The higher local T_{max}, which was indicative of the thermal decomposition of accretion products, was reported to be ∼80 °C, similar to the observed T_{max} value for $C_5H_{10}O_3$ and $C_5H_{12}O_4$, as shown in Figure 5. We also note, however, that the FIGAERO design used by Lopez-Hilfiker et al. (2016, ES&T) differs from commercial copies like ours, which could result in different desorption behaviors. In addition, a distinct multimodal thermogram, which is an indicator for thermal decomposition, was not observed in this work for $C_5H_{10}O_3$ and $C_5H_{12}O_4$. Nonetheless, the contribution of accretion products to the overall Cl−isoprene SOA mass is likely higher than Figure 4b would suggest, considering that thermal fragmentation occurs inside the FIGAERO-CIMS. Under high-NO_x conditions, negligible dimer concentrations were observed in the particle phase for isoprene−OH products.[71] It should be noted that these OH−isoprene dimer fractions were estimated from experiments under dry conditions, whereas lower aerosol pH and/or high RH (>50%) have been shown to enhance dimer formation.[72]

Under low-NO_x conditions, CHO and CHClO account for most (>90%) of the particulate mass observed by the I^--FIGAERO-CIMS. $C_5H_{4,6,8}O_{3-5}$ monomers and C_{6-8} dimers are among the most abundant CHO products, while $C_5H_{7-11}Cl_{1-2}O_{2-4}$ monomers are among the most abundant CHClO compounds, as shown in Table S1b. Under high-NO_x conditions, CHO accounts for over 50% of the observed particulate OA mass, with minor contribution by CHClO, CHNO, and CHClNO compounds. $C_5H_{8,10,12}O_{3-5}$ species are among the most abundant CHO compounds observed, with $C_5H_{12}O_4$ (e.g., isomers of methyltetrol) and $C_5H_{10}O_3$ (e.g., isomers of ISOPOOH and C_5-alkene triol) alone accounting for more than 10% of the observed SOA mass. Prominent but supposedly volatile species such as $C_2H_4O_3$ observed in the particle phase may be thermal decomposition products of accretion products. Compounds such as $C_5H_{12}O_5$ and $C_5H_{10}O_5$ (Figure S5) have also been identified as key particle-phase components of OH−ISOPOOH oxidation, accounting for as much as 65% of the non-IEPOX SOA mass under low-NO_x conditions together with other highly oxidized organic molecules such as $C_5H_{12}O_6$, $C_5H_{10}O_6$, and $C_5H_{10}O_7$,[69−73] which were not observed in Cl−isoprene SOA. Particulate $C_5H_{12}O_4$ and $C_5H_{12}O_5$ are traditionally attributed to the acid-catalyzed reactive uptake of IEPOX reaction pathways, though studies have reported non-IEPOX uptake, OH−isoprene oxidation pathways for them or their

https://doi.org/10.1021/acs.est.1c07048
Environ. Sci. Technol. 2022, 56, 9251−9264

isomers.[69−72,113] Caution should be exercised when using $C_5H_{12}O_4$ and $C_5H_{12}O_5$ as unique markers for IEPOX chemistry,[69−72,113] considering the possible Cl- and OH chemistry pathways, as well as potential interferences from the decomposition of accretion products during thermal volatilization-based analyses.

Under high-NO_x conditions, $(ONO)C_4H_7O_2$ and (ONO_2)-$C_5H_{7,9,11}O_{2-4}$ dominate the CHNO produced from Cl−isoprene oxidation. As a comparison, high-NO_x OH−isoprene SOA products consist primarily of $(ONO_2)C_5H_{7,9,11}O_{1-5}$ with $(ONO_2)C_5H_{11}O_4$ being the most abundant.[71] Using an average molecular weight for CHNO of approximately 200 g mol^{-1} based on FIGAERO measurements, the organic nitrates would account for ∼25% of the bulk SOA mass based on the NO_3 measurement by ACSM, which is consistent with the bulk CHNO contribution estimated using FIGAERO measurement alone (∼20%; Figure 4b and Table S1d). In comparison, the bulk composition measurement with the AMS suggests that organic nitrate can account for ∼40% of isoprene SOA mass under high-NO_x conditions.[71] Overall, the Cl−isoprene oxidation products have slightly fewer numbers of non-nitrate oxygen atoms (predominately 2−5) as compared to OH−isoprene oxidation products (predominately 4−6).[69−72,113]

In summary, we investigated the composition of Cl−isoprene SOA produced under low- and high-NO_x conditions for the first time, as well as the gas-phase composition using an I^--FIGAERO-CIMS. We note that product composition reported in this study is specific to our experimental conditions. For instance, the chamber radical concentration may not be representative of typical ambient conditions, where the elevated Cl concentration may bias the oxidation chemistry toward organic chloride formation and bimolecular reactions, underestimating the importance of isomerization pathways, e.g., autoxidation via intramolecular H-shift.[70] Furthermore, the organic nitrate yield has been shown to nonmonotonically vary with NO concentrations in OH−isoprene oxidations due to scavenging of first-generation RO_2 radicals.[71] Future studies should systematically explore the NO_x, Cl, and HO_x dependences of gas- and particle-phase yields for organics, organic nitrate, and/or chlorides from Cl−isoprene oxidation. Nonetheless, our results show that Cl-initiated oxidation readily produces multifunctional organic chloride compounds such as $C_5H_{11}ClO_3$, $C_5H_9ClO_3$, and $C_5H_9ClO_4$ that are consistently observed in both the gas and particle phases under low- and high-NO_x conditions, which may be candidates as tracers for Cl−isoprene oxidation chemistry in addition to isomers of CMBO (C_5H_7ClO). Some potential reaction pathways leading to the formation of dominant organic chloride products such as $C_5H_8Cl_2O_3$, $C_5H_9ClO_2$, $C_5H_9ClO_3$, $C_5H_{10}Cl_2O_2$, and $C_5H_{11}ClO_3$ are shown in Figure S6. It is interesting to note that, because of its high reaction rate coefficient with Cl radicals, isoprene may compete with other VOCs (e.g., α-pinene and toluene) and suppress overall SOA and HOM yields. At the same time, the scavenging of Cl radicals by isoprene may increase the overall gas- and/or particle-phase organic chloride production, considering that the Cl addition reaction is much more important in small alkenes[114] like isoprene (85%) compared to other VOCs such as alkanes and aromatics, where H-abstraction dominates and most Cl radicals are converted to HCl.[115] Our experimental and modeling results also indicate that OH−isoprene chemistry is an integral part of high-NO_x Cl−isoprene oxidation chemistry, accounting for up to 40% of total isoprene oxidation, with potentially greater importance under ambient conditions. Considerations of the (indirect) effects of Cl chemistry should therefore be taken into account. For instance, the importance of ambient chlorine chemistry may be underestimated due to the formation of nonchlorinated organic oxidation products, as well as the enhancement of non-Cl radical chemistry, which can result in indirect contribution to HOM and SOA productions. Given the importance of isoprene to air quality and recent reports of the elevated concentration of reactive chlorine species in polluted environments, our study provides timely insights into chemical processes occurring in anthropogenically influenced environments, which will impact urban air quality.

■ ASSOCIATED CONTENT

Supporting Information

The Supporting Information is available free of charge at https://pubs.acs.org/doi/10.1021/acs.est.1c07048.

Chamber model used; time series of ACSM measurements; time series of trace gases; time series of gas-phase oxidation products; and table of dominant gas- and particle-phase oxidation products (PDF)

■ AUTHOR INFORMATION

Corresponding Authors

Dongyu S. Wang − *McKetta Department of Chemical Engineering, University of Texas at Austin, Austin, Texas 78712, United States; Laboratory of Atmospheric Chemistry, Paul Scherrer Institute, 5232 Villigen, Switzerland*; Phone: +41 0563105842; Email: dongyu.wang@psi.ch

Lea Hildebrandt Ruiz − *McKetta Department of Chemical Engineering, University of Texas at Austin, Austin, Texas 78712, United States*; orcid.org/0000-0001-8378-1882; Phone: +01 5124714634; Email: lhr@utexas.edu

Authors

Catherine G. Masoud − *McKetta Department of Chemical Engineering, University of Texas at Austin, Austin, Texas 78712, United States*

Mrinali Modi − *McKetta Department of Chemical Engineering, University of Texas at Austin, Austin, Texas 78712, United States*

Complete contact information is available at: https://pubs.acs.org/10.1021/acs.est.1c07048

Author Contributions

§D.S.W. and C.G.M. contributed equally to this work. D.S.W., C.G.M., and L.H.R. designed the study. D.S.W. and C.G.M. performed the experiments and analyzed the data. M.M. performed the model simulations. All authors prepared the manuscript.

Notes

The authors declare no competing financial interest.

■ ACKNOWLEDGMENTS

This material is based on work supported, in part, by the Welch Foundation under grant Nos. F-1925-20170325 and F-1925-20200401, the National Science Foundation under grant No. 165362, and the European Union's Horizon 2020 research and innovation program under the Marie Skłodowska-Curie grant agreement No. 701647. The authors thank all sponsors

for their support and Leif G. Jahn for helpful discussions about the reaction mechanisms.

REFERENCES

(1) Cohen, A. J.; Brauer, M.; Burnett, R.; Anderson, H. R.; Frostad, J.; Estep, K.; Balakrishnan, K.; Brunekreef, B.; Dandona, L.; Dandona, R.; Feigin, V.; Freedman, G.; Hubbell, B.; Jobling, A.; Kan, H.; Knibbs, L.; Liu, Y.; Martin, R.; Morawska, L.; Pope, C. A.; Shin, H.; Straif, K.; Shaddick, G.; Thomas, M.; van Dingenen, R.; van Donkelaar, A.; Vos, T.; Murray, C. J. L.; Forouzanfar, M. H. Estimates and 25-Year Trends of the Global Burden of Disease Attributable to Ambient Air Pollution: An Analysis of Data from the Global Burden of Diseases Study 2015. *Lancet* **2017**, *389*, 1907−1918.

(2) Burnett, R.; Chen, H.; Szyszkowicz, M.; Fann, N.; Hubbell, B.; Pope, C. A.; Apte, J. S.; Brauer, M.; Cohen, A.; Weichenthal, S.; Coggins, J.; Di, Q.; Brunekreef, B.; Frostad, J.; Lim, S. S.; Kan, H.; Walker, K. D.; Thurston, G. D.; Hayes, R. B.; Lim, C. C.; Turner, M. C.; Jerrett, M.; Krewski, D.; Gapstur, S. M.; Diver, W. R.; Ostro, B.; Goldberg, D.; Crouse, D. L.; Martin, R. V.; Peters, P.; Pinault, L.; Tjepkema, M.; Van Donkelaar, A.; Villeneuve, P. J.; Miller, A. B.; Yin, P.; Zhou, M.; Wang, L.; Janssen, N. A. H.; Marra, M.; Atkinson, R. W.; Tsang, H.; Thach, T. Q.; Cannon, J. B.; Allen, R. T.; Hart, J. E.; Laden, F.; Cesaroni, G.; Forastiere, F.; Weinmayr, G.; Jaensch, A.; Nagel, G.; Concin, H.; Spadaro, J. V. Global Estimates of Mortality Associated with Longterm Exposure to Outdoor Fine Particulate Matter. *Proc. Natl. Acad. Sci. U.S.A.* **2018**, *115*, 9592−9597.

(3) Dockery, D. W.; Pope, C. A.; Xu, X.; Spengler, J. D.; Ware, J. H.; Fay, M. E.; Ferris, B. G.; Speizer, F. E. An Association between Air Pollution and Mortality in Six U.S. Cities. *N. Engl. J. Med.* **1993**, *329*, 1753−1759.

(4) Pope, C. A., III; Dockery, D. W. Health Effects of Fine Particulate Air Pollution: Lines That Connect. *J. Air Waste Manage. Assoc.* **2006**, *56*, 1368−1380.

(5) Nault, B. A.; Jo, D. S.; McDonald, B. C.; Campuzano-Jost, P.; Day, D. A.; Hu, W.; Schroder, J. C.; Allan, J.; Blake, D. R.; Canagaratna, M. R.; Coe, H.; Coggon, M. M.; Decarlo, P. F.; Diskin, G. S.; Dunmore, R.; Flocke, F.; Fried, A.; Gilman, J. B.; Gkatzelis, G.; Hamilton, J. F.; Hanisco, T. F.; Hayes, P. L.; Henze, D. K.; Hodzic, A.; Hopkins, J.; Hu, M.; Huey, L. G.; Jobson, B. T.; Kuster, W. C.; Lewis, A.; Li, M.; Liao, J.; Nawaz, M. O.; Pollack, I. B.; Peischl, J.; Rappenglück, B.; Reeves, C. E.; Richter, D.; Roberts, J. M.; Ryerson, T. B.; Shao, M.; Sommers, J. M.; Walega, J.; Warneke, C.; Weibring, P.; Wolfe, G. M.; Young, D. E.; Yuan, B.; Zhang, Q.; De Gouw, J. A.; Jimenez, J. L. Secondary Organic Aerosols from Anthropogenic Volatile Organic Compounds Contribute Substantially to Air Pollution Mortality. *Atmos. Chem. Phys.* **2021**, *21*, 11201−11224.

(6) McDonald, B. C.; de Gouw, J. A.; Gilman, J. B.; Jathar, S. H.; Akherati, A.; Cappa, C. D.; Jimenez1, J. L.; Lee-Taylor, J.; Hayes, P. L.; McKeen, S. A.; Cui, Y. Y.; Kim, S.-W.; Gentner, D. R.; Isaacman-VanWertz, G.; Goldstein, A. H.; Harley, R. A.; Frost, G. J.; Roberts, J. M.; Ryerson, T. B.; Trainer, M. Volatile Chemical Products Emerging as Largest Petrochemical Source of Urban Organic Emissions. *Science* **2017**, 760−764.

(7) Jimenez, J. L.; Canagaratna, M. R.; Donahue, N. M.; Prevot, A. S. H.; Zhang, Q.; Kroll, J. H.; DeCarlo, P. F.; Allan, J. D.; Coe, H.; Ng, N. L.; Aiken, A. C.; Docherty, K. S.; Ulbrich, I. M.; Grieshop, A. P.; Robinson, A. L.; Duplissy, J.; Smith, J. D.; Wilson, K. R.; Lanz, V. A.; Hueglin, C.; Sun, Y. L.; Tian, J.; Laaksonen, A.; Raatikainen, T.; Rautiainen, J.; Vaattovaara, P.; Ehn, M.; Kulmala, M.; Tomlinson, J. M.; Collins, D. R.; Cubison, M. J.; Dunlea, J.; Huffman, J. A.; Onasch, T. B.; Alfarra, M. R.; Williams, P. I.; Bower, K.; Kondo, Y.; Schneider, J.; Drewnick, F.; Borrmann, S.; Weimer, S.; Demerjian, K.; Salcedo, D.; Cottrell, L.; Griffin, R.; Takami, A.; Miyoshi, T.; Hatakeyama, S.; Shimono, A.; Sun, J. Y.; Zhang, Y. M.; Dzepina, K.; Kimmel, J. R.; Sueper, D.; Jayne, J. T.; Herndon, S. C.; Trimborn, A. M.; Williams, L. R.; Wood, E. C.; Middlebrook, A. M.; Kolb, C. E.; Baltensperger, U.; Worsnop, D. R. Evolution of Organic Aerosols in the Atmosphere. *Science* **2009**, *326*, 1525−1529.

(8) Hodzic, A.; Campuzano-Jost, P.; Bian, H.; Chin, M.; Colarco, P.; Day, D.; Froyd, K.; Heinold, B.; Jo, D.; Katich, J.; Kodros, J.; Nault, B.; Pierce, J.; Ray, E.; Schacht, J.; Schill, G.; Schroder, J.; Schwarz, J.; Sueper, D.; Tegen, I.; Tilmes, S.; Tsigaridis, K.; Yu, P.; Jimenez, J. Characterization of Organic Aerosol across the Global Remote Troposphere: A Comparison of ATom Measurements and Global Chemistry Models. *Atmos. Chem. Phys. Discuss.* **2019**, 1−56.

(9) Pai, S. J.; Heald, C.; Pierce, J.; Farina, S.; Marais, E.; Jimenez, J.; Campuzano-Jost, P.; Nault, B.; Middlebrook, A.; Coe, H.; Shilling, J.; Bahreini, R.; Dingle, J.; Vu, K. An Evaluation of Global Organic Aerosol Schemes Using Airborne Observations. *Atmos. Chem. Phys. Discuss.* **2019**, 1−39.

(10) De Gouw, J.; Jimenez, J. L. Organic Aerosols in the Earth's Atmosphere. *Environ. Sci. Technol.* **2009**, *43*, 7614−7618.

(11) Priestley, M.; le Breton, M.; Bannan, T. J.; Worrall, S. D.; Bacak, A.; Smedley, A. R. D.; Reyes-Villegas, E.; Mehra, A.; Allan, J.; Webb, A. R.; Shallcross, D. E.; Coe, H.; Percival, C. J. Observations of Organic and Inorganic Chlorinated Compounds and Their Contribution to Chlorine Radical Concentrations in an Urban Environment in Northern Europe during the Wintertime. *Atmos. Chem. Phys.* **2018**, *18*, 13481−13493.

(12) Choi, M. S.; Qiu, X.; Zhang, J.; Wang, S.; Li, X.; Sun, Y.; Chen, J.; Ying, Q. Study of Secondary Organic Aerosol Formation from Chlorine Radical-Initiated Oxidation of Volatile Organic Compounds in a Polluted Atmosphere Using a 3D Chemical Transport Model. *Environ. Sci. Technol.* **2020**, *54*, 13409.

(13) Wang, X.; Jacob, D. J.; Fu, X.; Wang, T.; Le Breton, M.; Hallquist, M.; Liu, Z.; Mcduffie, E. E.; Liao, H. Effects of Anthropogenic Chlorine on PM2.5and Ozone Air Quality in China. *Environ. Sci. Technol.* **2020**, *54*, 9908−9916.

(14) Fan, X.; Cai, J.; Yan, C.; Zhao, J.; Guo, Y.; Li, C.; Dällenbach, K. R.; Zheng, F.; Lin, Z.; Chu, B.; Wang, Y.; Dada, L.; Zha, Q.; Du, W.; Kontkanen, J.; Kurtén, T.; Iyer, S.; Kujansuu, J. T.; Petäjä, T.; Worsnop, D. R.; Kerminen, V.-M.; Liu, Y.; Bianchi, F.; Tham, Y. J.; Yao, L.; Kulmala, M. Atmospheric Gaseous Hydrochloric and Hydrobromic Acid in Urban Beijing, China: Detection, Source Identification and Potential Atmospheric Impacts. *Atmos. Chem. Phys.* **2021**, *21*, 11437−11452.

(15) Mielke, L. H.; Furgeson, A.; Osthoff, H. D. Observation of ClNO 2 in a Mid-Continental Urban Environment. *Environ. Sci. Technol.* **2011**, *45*, 8889−8896.

(16) Haskins, J. D.; Lopez-Hilfiker, F. D.; Lee, B. H.; Shah, V.; Wolfe, G. M.; DiGangi, J.; Fibiger, D.; McDuffie, E. E.; Veres, P.; Schroder, J. C.; Campuzano-Jost, P.; Day, D. A.; Jimenez, J. L.; Weinheimer, A.; Sparks, T.; Cohen, R. C.; Campos, T.; Sullivan, A.; Guo, H.; Weber, R.; Dibb, J.; Green, J.; Fiddler, M.; Bililign, S.; Jaeglé, L.; Brown, S. S.; Thornton, J. A. Anthropogenic Control Over Wintertime Oxidation of Atmospheric Pollutants. *Geophys. Res. Lett.* **2019**, *46*, 14826−14835.

(17) Li, Q.; Badia, A.; Wang, T.; Sarwar, G.; Fu, X.; Zhang, L.; Zhang, Q.; Fung, J.; Cuevas, C. A.; Wang, S.; Zhou, B.; Saiz-Lopez, A. Potential Effect of Halogens on Atmospheric Oxidation and Air Quality in China. *J. Geophys. Res.: Atmos.* **2020**, *125*, No. e2019JD032058.

(18) Wang, X.; Jacob, D.; Eastham, S.; Sulprizio, M.; Zhu, L.; Chen, Q.; Alexander, B.; Sherwen, T.; Evans, M.; Lee, B.; Haskins, J.; Lopez-Hilfiker, F.; Thornton, J.; Huey, G.; Liao, H. The Role of Chlorine in Tropospheric Chemistry. *Atmos. Chem. Phys. Discuss.* **2018**, 1−40.

(19) Gani, S.; Bhandari, S.; Seraj, S.; Wang, D. S.; Patel, K.; Soni, P.; Arub, Z.; Habib, G.; Hildebrandt Ruiz, L.; Apte, J. Submicron Aerosol Composition in the World's Most Polluted Megacity: The Delhi Aerosol Supersite Campaign. *Atmos. Chem. Phys. Discuss.* **2018**, *5*, 1−33.

(20) Saiz-Lopez, A.; von Glasow, R. Reactive Halogen Chemistry in the Troposphere. *Chem. Soc. Rev.* **2012**, *41*, 6448.

(21) Wingenter, O. W.; Blake, D. R.; Blake, N. J.; Sive, B. C.; Rowland, F. S.; Atlas, E.; Flocke, F. Tropospheric Hydroxyl and Atomic Chlorine Concentrations, and Mixing Timescales Determined

https://doi.org/10.1021/acs.est.1c07048
Environ. Sci. Technol. 2022, 56, 9251−9264

from Hydrocarbon and Halocarbon Measurements Made over the Southern Ocean. *J. Geophys. Res.* **1999**, *104*, 21819.
(22) Wingenter, O. W.; Sive, B. C.; Blake, N. J.; Blake, D. R.; Rowland, F. S. Atomic Chlorine Concentrations Derived from Ethane and Hydroxyl Measurements over the Equatorial Pacific Ocean: Implication for Dimethyl Sulfide and Bromine Monoxide. *J. Geophys. Res.* **2005**, *110*, No. D20308.
(23) Le Breton, M.; Hallquist, Å. M.; Kant Pathak, R.; Simpson, D.; Wang, Y.; Johansson, J.; Zheng, J.; Yang, Y.; Shang, D.; Wang, H.; Liu, Q.; Chan, C.; Wang, T.; Bannan, T. J.; Priestley, M.; Percival, C. J.; Shallcross, D. E.; Lu, K.; Guo, S.; Hu, M.; Hallquist, M. Chlorine Oxidation of VOCs at a Semi-Rural Site in Beijing: Significant Chlorine Liberation from ClNO2 and Subsequent Gas- A Nd Particle-Phase Cl-VOC Production. *Atmos. Chem. Phys.* **2018**, *18*, 13013−13030.
(24) McNamara, S. M.; Raso, A. R. W.; Wang, S.; Thanekar, S.; Boone, E. J.; Kolesar, K. R.; Peterson, P. K.; Simpson, W. R.; Fuentes, J. D.; Shepson, P. B.; Pratt, K. A. Springtime Nitrogen Oxide-Influenced Chlorine Chemistry in the Coastal Arctic. *Environ. Sci. Technol.* **2019**, *53*, 8057−8067.
(25) Liu, X.; Qu, H.; Huey, L. G.; Wang, Y.; Sjostedt, S.; Zeng, L.; Lu, K.; Wu, Y.; Hu, M.; Shao, M.; Zhu, T.; Zhang, Y. High Levels of Daytime Molecular Chlorine and Nitryl Chloride at a Rural Site on the North China Plain. *Environ. Sci. Technol.* **2017**, *51*, 9588−9595.
(26) Thornton, J. A.; Kercher, J. P.; Riedel, T. P.; Wagner, N. L.; Cozic, J.; Holloway, J. S.; Dubé, W. P.; Wolfe, G. M.; Quinn, P. K.; Middlebrook, A. M.; Alexander, B.; Brown, S. S. A Large Atomic Chlorine Source Inferred from Mid-Continental Reactive Nitrogen Chemistry. *Nature* **2010**, *464*, 271−274.
(27) Riedel, T. P.; Wolfe, G. M.; Danas, K. T.; Gilman, J. B.; Kuster, W. C.; Bon, D. M.; Vlasenko, A.; Li, S.-M.; Williams, E. J.; Lerner, B. M.; Veres, P. R.; Roberts, J. M.; Holloway, J. S.; Lefer, B.; Brown, S. S.; Thornton, J. A. An MCM Modeling Study of Nitryl Chloride (ClNO2) Impacts on Oxidation, Ozone Production and Nitrogen Oxide Partitioning in Polluted Continental Outflow. *Atmos. Chem. Phys.* **2014**, *14*, 3789−3800.
(28) Young, C. J.; Washenfelder, R. A.; Edwards, P. M.; Parrish, D. D.; Gilman, J. B.; Kuster, W. C.; Mielke, L. H.; Osthoff, H. D.; Tsai, C.; Pikelnaya, O.; Stutz, J.; Veres, P. R.; Roberts, J. M.; Griffith, S.; Dusanter, S.; Stevens, P. S.; Flynn, J.; Grossberg, N.; Lefer, B.; Holloway, J. S.; Peischl, J.; Ryerson, T. B.; Atlas, E. L.; Blake, D. R.; Brown, S. S. Chlorine as a Primary Radical: Evaluation of Methods to Understand Its Role in Initiation of Oxidative Cycles. *Atmos. Chem. Phys.* **2014**, *14*, 3427−3440.
(29) Tham, Y. J.; Wang, Z.; Li, Q.; Yun, H.; Wang, W.; Wang, X.; Xue, L.; Lu, K.; Ma, N.; Bohn, B.; Li, X.; Kecorius, S.; Größ, J.; Shao, M.; Wiedensohler, A.; Zhang, Y.; Wang, T. Significant Concentrations of Nitryl Chloride Sustained in the Morning: Investigations of the Causes and Impacts on Ozone Production in a Polluted Region of Northern China. *Atmos. Chem. Phys.* **2016**, *16*, 14959−14977.
(30) Wang, Y.; Hu, M.; Guo, S.; Wang, Y.; Zheng, J.; Yang, Y.; Zhu, W.; Tang, R.; Li, X.; Liu, Y.; Le Breton, M.; Du, Z.; Shang, D.; Wu, Y.; Wu, Z.; Song, Y.; Lou, S.; Hallquist, M.; Yu, J. The Secondary Formation of Organosulfates under the Interactions between Biogenic Emissions and Anthropogenic Pollutants in Summer of Beijing. *Atmos. Chem. Phys.* **2018**, *7*, 10693−10713.
(31) Yun, H.; Wang, W.; Wang, T.; Xia, M.; Yu, C.; Wang, Z.; Poon, S. C. N.; Yue, D.; Zhou, Y. Nitrate Formation from Heterogeneous Uptake of Dinitrogen Pentoxide during a Severe Winter Haze in Southern China. *Atmos. Chem. Phys.* **2018**, *18*, 17515−17527.
(32) Ahern, A. T.; Goldberger, L.; Jahl, L.; Thornton, J.; Sullivan, R. C. Production of N2O5 and ClNO2 through Nocturnal Processing of Biomass-Burning Aerosol. *Environ. Sci. Technol.* **2018**, *52*, 550−559.
(33) Finlayson-Pitts, B. J.; Ezell, M. J.; Pitts, J. N. Formation of Chemically Active Chlorine Compounds by Reactions of Atmospheric NaCl Particles with Gaseous N2O5 and ClONO2. *Nature* **1989**, *337*, 241−244.
(34) Bannan, T. J.; Khan, M. A. H.; Le Breton, M.; Priestley, M.; Worrall, S. D.; Bacak, A.; Marsden, N. A.; Lowe, D.; Pitt, J.; Allen, G.; Topping, D.; Coe, H.; McFiggans, G.; Shallcross, D. E.; Percival, C. J. A Large Source of Atomic Chlorine From ClNO2 Photolysis at a U.K. Landfill Site. *Geophys. Res. Lett.* **2019**, *46*, 8508−8516.
(35) Mattila, J. M.; Arata, C.; Wang, C.; Katz, E. F.; Abeleira, A.; Zhou, Y.; Zhou, S.; Goldstein, A. H.; Abbatt, J. P. D.; Decarlo, P. F.; Farmer, D. K. Dark Chemistry during Bleach Cleaning Enhances Oxidation of Organics and Secondary Organic Aerosol Production Indoors. *Environ. Sci. Technol. Lett.* **2020**, *7*, 795−801.
(36) Couto, M.; Bernard, A.; Delgado, L.; Drobnic, F.; Kurowski, M.; Moreira, A.; Rodrigues-Alves, R.; Rukhadze, M.; Seys, S.; Wiszniewska, M.; Quirce, S. Health Effects of Exposure to Chlorination By-products in Swimming Pools. *Allergy* **2021**, *76*, 3257.
(37) Lakey, P. S. J.; Won, Y.; Shaw, D.; Østerstrøm, F. F.; Mattila, J.; Reidy, E.; Bottorff, B.; Rosales, C.; Wang, C.; Ampollini, L.; Zhou, S.; Novoselac, A.; Kahan, T. F.; DeCarlo, P. F.; Abbatt, J. P. D.; Stevens, P. S.; Farmer, D. K.; Carslaw, N.; Rim, D.; Shiraiwa, M. Spatial and Temporal Scales of Variability for Indoor Air Constituents. *Commun. Chem.* **2021**, *4*, No. 110.
(38) Mattila, J. M.; Lakey, P. S. J.; Shiraiwa, M.; Wang, C.; Abbatt, J. P. D.; Arata, C.; Goldstein, A. H.; Ampollini, L.; Katz, E. F.; Decarlo, P. F.; Zhou, S.; Kahan, T. F.; Cardoso-Saldaña, F. J.; Ruiz, L. H.; Abeleira, A.; Boedicker, E. K.; Vance, M. E.; Farmer, D. K. Multiphase Chemistry Controls Inorganic Chlorinated and Nitrogenated Compounds in Indoor Air during Bleach Cleaning. *Environ. Sci. Technol.* **2020**, *54*, 1730−1739.
(39) Schwartz-Narbonne, H.; Wang, C.; Zhou, S.; Abbatt, J. P. D.; Faust, J. Heterogeneous Chlorination of Squalene and Oleic Acid. *Environ. Sci. Technol.* **2018**, 1217.
(40) Wang, C.; Collins, D. B.; Abbatt, J. P. D. Indoor Illumination of Terpenes and Bleach Emissions Leads to Particle Formation and Growth. *Environ. Sci. Technol.* **2019**, *53*, 11792−11800.
(41) Sherwen, T.; Evans, M. J.; Sommariva, R.; Hollis, L. D. J.; Ball, S. M.; Monks, P. S.; Reed, C.; Carpenter, L. J.; Lee, J. D.; Forster, G.; Bandy, B.; Reeves, C. E.; Bloss, W. J. Effects of Halogens on European Air-Quality. *Faraday Discuss.* **2017**, *200*, 75−100.
(42) Wennberg, P. O.; Bates, K. H.; Crounse, J. D.; Dodson, L. G.; McVay, R. C.; Mertens, L. A.; Nguyen, T. B.; Praske, E.; Schwantes, R. H.; Smarte, M. D.; St Clair, J. M.; Teng, A. P.; Zhang, X.; Seinfeld, J. H. Gas-Phase Reactions of Isoprene and Its Major Oxidation Products. *Chem. Rev.* **2018**, *118*, 3337−3390.
(43) Dhulipala, S. V.; Bhandari, S.; Hildebrandt Ruiz, L. Formation of Oxidized Organic Compounds from Cl-Initiated Oxidation of Toluene. *Atmos. Environ.* **2019**, *199*, 265−273.
(44) Cai, X.; Ziemba, L. D.; Griffin, R. J. Secondary Aerosol Formation from the Oxidation of Toluene by Chlorine Atoms. *Atmos. Environ.* **2008**, *42*, 7348−7359.
(45) Wang, D. S.; Hildebrandt Ruiz, L. Secondary Organic Aerosol from Chlorine-Initiated Oxidation of Isoprene. *Atmos. Chem. Phys.* **2017**, *17*, 13491−13508.
(46) Wang, D. S.; Hildebrandt Ruiz, L. Chlorine-Initiated Oxidation of n-Alkanes under High-NOx Conditions: Insights into Secondary Organic Aerosol Composition and Volatility Using a FIGAERO−CIMS. *Atmos. Chem. Phys.* **2018**, *18*, 15535−15553.
(47) Jahn, L. G.; Wang, D. S.; Dhulipala, S. V.; Ruiz, L. H. Gas-Phase Chlorine Radical Oxidation of Alkanes: Effects of Structural Branching, NO x, and Relative Humidity Observed during Environmental Chamber Experiments. *J. Phys. Chem. A* **2021**, *125*, 7303.
(48) Cai, X.; Griffin, R. J. Secondary Aerosol Formation from the Oxidation of Biogenic Hydrocarbons by Chlorine Atoms. *J. Geophys. Res.* **2006**, *111*, No. D14206.
(49) Riva, M.; Healy, R. M.; Flaud, P. M.; Perraudin, E.; Wenger, J. C.; Villenave, E. Gas- and Particle-Phase Products from the Chlorine-Initiated Oxidation of Polycyclic Aromatic Hydrocarbons. *J. Phys. Chem. A* **2015**, *119*, 11170−11181.
(50) Masoud, C. G.; Ruiz, L. H. Chlorine-Initiated Oxidation of α-Pinene: Formation of Secondary Organic Aerosol and Highly Oxygenated Organic Molecules. *ACS Earth Space Chem.* **2021**, *5*, 2307.

https://doi.org/10.1021/acs.est.1c07048
Environ. Sci. Technol. 2022, 56, 9251−9264

(51) Nordmeyer, T.; Wang, W.; Ragains, M. L.; Finlayson-Pitts, B. J.; Spicer, C. W.; Plastridge, R. A. Unique Products of the Reaction of Isoprene with Atomic Chlorine: Potential Markers of Chlorine Atom Chemistry. *Geophys. Res. Lett.* **1997**, *24*, 1615−1618.
(52) Riemer, D. D.; Apel, E. C.; Orlando, J. J.; Tyndall, G. S.; Brune, W. H.; Williams, E. J.; Lonneman, W. A.; Neece, J. D. Unique Isoprene Oxidation Products Demonstrate Chlorine Atom Chemistry Occurs in the Houston, Texas Urban Area. *J. Atmos. Chem.* **2008**, *61*, 227−242.
(53) Wang, W.; Finlayson-Pitts, B. J. Unique Markers of Chlorine Atom Chemistry in Coastal Urban Areas: The Reaction with 1,3-Butadiene in Air at Room Temperature. *J. Geophys. Res.: Atmos.* **2001**, *106*, 4939−4958.
(54) Tanaka, P. L.; Riemer, D. D.; Chang, S.; Yarwood, G.; McDonald-Buller, E. C.; Apel, E. C.; Orlando, J. J.; Silva, P. J.; Jimenez, J. L.; Canagaratna, M. R.; Neece, J. D.; Mullins, C. B.; Allen, D. T. Direct Evidence for Chlorine-Enhanced Urban Ozone Formation in Houston, Texas. *Atmos. Environ.* **2003**, *37*, 1393−1400.
(55) Guenther, A. B.; Jiang, X.; Heald, C. L.; Sakulyanontvittaya, T.; Duhl, T.; Emmons, L. K.; Wang, X. The Model of Emissions of Gases and Aerosols from Nature Version 2.1 (MEGAN2.1): An Extended and Updated Framework for Modeling Biogenic Emissions. *Geosci. Model Dev.* **2012**, *5*, 1471−1492.
(56) Guenther, A.; Karl, T.; Harley, P.; Wiedinmyer, C.; Palmer, P. I.; Geron, C. Estimates of Global Terrestrial Isoprene Emissions Using MEGAN (Model of Emissions of Gases and Aerosols from Nature. *Atmos. Chem. Phys.* **2006**, *6*, 3181−3210.
(57) Kashyap, P.; Kumar, A.; Kumar, R. P.; Kumar, K. Biogenic and Anthropogenic Isoprene Emissions in the Subtropical Urban Atmosphere of Delhi. *Atmos. Pollut. Res.* **2019**, *10*, 1691−1698.
(58) Von Schneidemesser, E.; Monks, P. S.; Gros, V.; Gauduin, J.; Sanchez, O. How Important Is Biogenic Isoprene in an Urban Environment? A Study in London and Paris. *Geophys. Res. Lett.* **2011**, *38*, No. L19804.
(59) Khan, M. A. H.; Schlich, B. L.; Jenkin, M. E.; Shallcross, B. M. A.; Moseley, K.; Walker, C.; Morris, W. C.; Derwent, R. G.; Percival, C. J.; Shallcross, D. E. A Two-Decade Anthropogenic and Biogenic Isoprene Emissions Study in a London Urban Background and a London Urban Traffic Site. *Atmosphere* **2018**, *9*, No. 387.
(60) Dunker, A. M.; Koo, B.; Yarwood, G. Ozone Sensitivity to Isoprene Chemistry and Emissions and Anthropogenic Emissions in Central California. *Atmos. Environ.* **2016**, *145*, 326−337.
(61) Kanakidou, M.; Seinfeld, J. H.; Pandis, S. N.; Barnes, I.; Dentener, F. J.; Facchini, M. C.; Van Dingenen, R.; Ervens, B.; Nenes, A.; Nielsen, C. J.; Swietlicki, E.; Putaud, J. P.; Balkanski, Y.; Fuzzi, S.; Horth, J.; Moortgat, G. K.; Winterhalter, R.; Myhre, C. E. L.; Tsigaridis, K.; Vignati, E.; Stephanou, E. G.; Wilson, J. Organic Aerosol and Global Climate Modelling: A Review. *Atmos. Chem. Phys.* **2005**, *5*, 1053−1123.
(62) Doyle, M.; Sexton, K. G.; Jeffries, H.; Bridge, K.; Jaspers, I. Effects of 1,3-Butadiene, Isoprene, and Their Photochemical Degradation Products on Human Lung Cells. *Environ. Health Perspect.* **2004**, *112*, 1488−1495.
(63) Surratt, J. D.; Chan, A. W.; Eddingsaas, N. C.; Chan, M.; Loza, C. L.; Kwan, A. J.; Hersey, S. P.; Flagan, R. C.; Wennberg, P. O.; Seinfeld, J. H. Reactive Intermediates Revealed in Secondary Organic Aerosol Formation from Isoprene. *Proc. Natl. Acad. Sci. U.S.A.* **2010**, *107*, 6640−6645.
(64) Lin, Y.-H.; Zhang, Z.; Docherty, K. S.; Zhang, H.; Budisulistiorini, S. H.; Rubitschun, C. L.; Shaw, S. L.; Knipping, E. M.; Edgerton, E. S.; Kleindienst, T. E.; Gold, A.; Surratt, J. D. Isoprene Epoxydiols as Precursors to Secondary Organic Aerosol Formation: Acid-Catalyzed Reactive Uptake Studies with Authentic Compounds. *Environ. Sci. Technol.* **2012**, *46*, 250−258.
(65) Nguyen, T. B.; Crounse, J. D.; Schwantes, R. H.; Teng, A. P.; Bates, K. H.; Zhang, X.; St Clair, J. M.; Brune, W. H.; Tyndall, G. S.; Keutsch, F. N.; Seinfeld, J. H.; Wennberg, P. O. Overview of the Focused Isoprene EXperiment at the California Institute of Technology (FIXCIT): Mechanistic Chamber Studies on the Oxidation of Biogenic Compounds. *Atmos. Chem. Phys.* **2014**, *14*, 13531−13549.
(66) Gaston, C. J.; Riedel, T. P.; Zhang, Z.; Gold, A.; Surratt, J. D.; Thornton, J. A. Reactive Uptake of an Isoprene-Derived Epoxydiol to Submicron Aerosol Particles. *Environ. Sci. Technol.* **2014**, *48*, 11178−11186.
(67) Paulot, F.; Crounse, J. D.; Kjaergaard, H. G.; Kurten, A.; St Clair, J. M.; Seinfeld, J. H.; Wennberg, P. O. Unexpected Epoxide Formation in the Gas-Phase Photooxidation of Isoprene. *Science* **2009**, *325*, 730−733.
(68) Riva, M.; Chen, Y.; Zhang, Y.; Lei, Z.; Olson, N. E.; Boyer, H. C.; Narayan, S.; Yee, L. D.; Green, H. S.; Cui, T.; Zhang, Z.; Baumann, K.; Fort, M.; Edgerton, E.; Budisulistiorini, S. H.; Rose, C. A.; Ribeiro, I. O.; Oliveira, R. L. E.; Dos Santos, E. O.; Machado, C. M. D.; Szopa, S.; Zhao, Y.; Alves, E. G.; De Sá, S. S.; Hu, W.; Knipping, E. M.; Shaw, S. L.; Duvoisin Junior, S.; De Souza, R. A. F.; Palm, B. B.; Jimenez, J. L.; Glasius, M.; Goldstein, A. H.; Pye, H. O. T.; Gold, A.; Turpin, B. J.; Vizuete, W.; Martin, S. T.; Thornton, J. A.; Dutcher, C. S.; Ault, A. P.; Surratt, J. D. Increasing Isoprene Epoxydiol-to-Inorganic Sulfate Aerosol Ratio Results in Extensive Conversion of Inorganic Sulfate to Organosulfur Forms: Implications for Aerosol Physicochemical Properties. *Environ. Sci. Technol.* **2019**, *53*, 8682−8694.
(69) Krechmer, J. E.; Coggon, M. M.; Massoli, P.; Nguyen, T. B.; Crounse, J. D.; Hu, W.; Day, D. A.; Tyndall, G. S.; Henze, D. K.; Rivera-Rios, J. C.; Nowak, J. B.; Kimmel, J. R.; Mauldin, R. L.; Stark, H.; Jayne, J. T.; Sipila, M.; Junninen, H.; St Clair, J. M.; Zhang, X.; Feiner, P. A.; Zhang, L.; Miller, D. O.; Brune, W. H.; Keutsch, F. N.; Wennberg, P. O.; Seinfeld, J. H.; Worsnop, D. R.; Jimenez, J. L.; Canagaratna, M. R. Formation of Low Volatility Organic Compounds and Secondary Organic Aerosol from Isoprene Hydroxyhydroperoxide Low-NO Oxidation. *Environ. Sci. Technol.* **2015**, *49*, 10330−10339.
(70) D'Ambro, E. L.; Møller, K. H.; Lopez-Hilfiker, F. D.; Schobesberger, S.; Liu, J.; Shilling, J. E.; Lee, B. H.; Kjaergaard, H. G.; Thornton, J. A. Isomerization of Second-Generation Isoprene Peroxy Radicals: Epoxide Formation and Implications for Secondary Organic Aerosol Yields. *Environ. Sci. Technol.* **2017**, *51*, 4978−4987.
(71) D'Ambro, E. L.; Lee, B. H.; Liu, J.; Shilling, J. E.; Gaston, C. J.; Lopez-Hilfiker, F. D.; Schobesberger, S.; Zaveri, R. A.; Mohr, C.; Lutz, A.; Zhang, Z.; Gold, A.; Surratt, J. D.; Rivera-Rios, J. C.; Keutsch, F. N.; Thornton, J. A. Molecular Composition and Volatility of Isoprene Photochemical Oxidation Secondary Organic Aerosol under Low- and High-NOx Conditions. *Atmos. Chem. Phys.* **2017**, *17*, 159−174.
(72) Riva, M.; Budisulistiorini, S. H.; Chen, Y.; Zhang, Z.; D'Ambro, E. L.; Zhang, X.; Gold, A.; Turpin, B. J.; Thornton, J. A.; Canagaratna, M. R.; Surratt, J. D. Chemical Characterization of Secondary Organic Aerosol from Oxidation of Isoprene Hydroxyhydroperoxides. *Environ. Sci. Technol.* **2016**, *50*, 9889−9899.
(73) Liu, J.; D'Ambro, E. L.; Lee, B. H.; Lopez-Hilfiker, F. D.; Zaveri, R. A.; Rivera-Rios, J. C.; Keutsch, F. N.; Iyer, S.; Kurten, T.; Zhang, Z.; Gold, A.; Surratt, J. D.; Shilling, J. E.; Thornton, J. A. Efficient Isoprene Secondary Organic Aerosol Formation from a Non-IEPOX Pathway. *Environ. Sci. Technol.* **2016**, *50*, 9872−9880.
(74) Kiendler-Scharr, A.; Wildt, J.; Dal Maso, M.; Hohaus, T.; Kleist, E.; Mentel, T. F.; Tillmann, R.; Uerlings, R.; Schurr, U.; Wahner, A. New Particle Formation in Forests Inhibited by Isoprene Emissions. *Nature* **2009**, *461*, 381−384.
(75) Mcfiggans, G.; Mentel, T. F.; Wildt, J.; Pullinen, I.; Kang, S.; Kleist, E.; Schmitt, S.; Springer, M.; Tillmann, R.; Wu, C.; Zhao, D.; Hallquist, M.; Faxon, C.; Le Breton, M.; Hallquist, A. M.; Simpson, D.; Bergstro, R.; Jenkin, M. E.; Ehn, M.; Thornton, J. A.; Alfarra, M. R.; Bannan, T. J.; Percival, C. J.; Priestley, M.; Topping, D.; Kiendler-Scharr, A. Secondary Organic Aerosol Reduced by Mixture of Atmospheric Vapours. *Nature* **2019**, *565*, 587−593.
(76) Li, K.; Zhang, X.; Zhao, B.; Bloss, W. J.; Lin, C.; White, S.; Yu, H.; Chen, L.; Geng, C.; Yang, W.; Azzi, M.; George, C.; Bai, Z. Suppression of Anthropogenic Secondary Organic Aerosol Formation by Isoprene. *npj Clim. Atmos. Sci.* **2022**, *5*, No. 12.

https://doi.org/10.1021/acs.est.1c07048
Environ. Sci. Technol. 2022, 56, 9251−9264

(77) Ragains, M. L.; Finlayson-Pitts, B. J. Kinetics and Mechanism of the Reaction of Cl Atoms with 2-Methyl-1,3-Butadiene (Isoprene) at 298 K. *J. Phys. Chem. A* **1997**, *101*, 1509−1517.
(78) Fantechi, G.; Jensen, N. R.; Saastad, O.; Hjorth, J.; Peeters, J. Reactions of Cl Atoms with Selected VOCs: Kinetics, Products and Mechanisms. *J. Atmos. Chem.* **1998**, *31*, 247−267.
(79) Guo, X.; Ma, F.; Liu, C.; Niu, J.; He, N.; Chen, J.; Xie, H. B. Atmospheric Oxidation Mechanism and Kinetics of Isoprene Initiated by Chlorine Radicals: A Computational Study. *Sci. Total Environ.* **2020**, *712*, No. 136330.
(80) Crounse, J. D.; Paulot, F.; Kjaergaard, H. G.; Wennberg, P. O. Peroxy Radical Isomerization in the Oxidation of Isoprene. *Phys. Chem. Chem. Phys.* **2011**, *13*, 13607−13613.
(81) Orlando, J. J.; Tyndall, G. S.; Apel, E. C.; Riemer, D. D.; Paulson, S. E. Rate Coefficients and Mechanisms of the Reaction of Cl-Atoms with a Series of Unsaturated Hydrocarbons under Atmospheric Conditions. *Int. J. Chem. Kinet.* **2003**, *35*, 334−353.
(82) Bean, J. K.; Hildebrandt Ruiz, L. Gas−Particle Partitioning and Hydrolysis of Organic Nitrates Formed from the Oxidation of α-Pinene in Environmental Chamber Experiments. *Atmos. Chem. Phys.* **2016**, *16*, 2175−2184.
(83) Carter, W. P. L.; Cocker, D. R.; Fitz, D. R.; Malkina, I. L.; Bumiller, K.; Sauer, C. G.; Pisano, J. T.; Bufalino, C.; Song, C. A New Environmental Chamber for Evaluation of Gas-Phase Chemical Mechanisms and Secondary Aerosol Formation. *Atmos. Environ.* **2005**, *39*, 7768−7788.
(84) Carter, W. P. L.; Cocker, D. R.; Fitz, D. R.; Malkina, I. L.; Bumiller, K.; Sauer, C. G.; Pisano, J. T.; Bufalino, C.; Song, C. A New Environmental Chamber for Evaluation of Gas-Phase Chemical Mechanisms and Secondary Aerosol Formation. *Atmos. Environ.* **2005**, *39*, 7768−7788.
(85) Alfarra, M. R. Insights into Atmospheric Organic Aerosols Using an Aerosol Mass Spectrometer. Ph.D. Thesis, University of Manchester: U.K., 2004.
(86) Tobler, A. K.; Skiba, A.; Wang, D. S.; Croteau, P.; Styszko, K.; Jarosław, N. Improved Chloride Quantification in Quadrupole Aerosol Chemical Speciation Monitors (Q-ACSMs). *Atmos. Meas. Tech.* **2020**, 5293−5301.
(87) Freney, E.; Zhang, Y.; Croteau, P.; Amodeo, T.; Williams, L.; Truong, F.; Petit, J. E.; Sciare, J.; Sarda-Esteve, R.; Bonnaire, N.; Arumae, T.; Aurela, M.; Bougiatioti, A.; Mihalopoulos, N.; Coz, E.; Artinano, B.; Crenn, V.; Elste, T.; Heikkinen, L.; Poulain, L.; Wiedensohler, A.; Herrmann, H.; Priestman, M.; Alastuey, A.; Stavroulas, I.; Tobler, A.; Vasilescu, J.; Zanca, N.; Canagaratna, M.; Carbone, C.; Flentje, H.; Green, D.; Maasikmets, M.; Marmureanu, L.; Minguillon, M. C.; Prevot, A. S. H.; Gros, V.; Jayne, J.; Favez, O. The Second ACTRIS Inter-Comparison (2016) for Aerosol Chemical Speciation Monitors (ACSM): Calibration Protocols and Instrument Performance Evaluations. *Aerosol Sci. Technol.* **2019**, *53*, 830−842.
(88) Ng, N. L.; Herndon, S. C.; Trimborn, A.; Canagaratna, M. R.; Croteau, P. L.; Onasch, T. B.; Sueper, D.; Worsnop, D. R.; Zhang, Q.; Sun, Y. L.; Jayne, J. T. An Aerosol Chemical Speciation Monitor (ACSM) for Routine Monitoring of the Composition and Mass Concentrations of Ambient Aerosol. *Aerosol Sci. Technol.* **2011**, *45*, 780−794.
(89) Hildebrandt, L.; Donahue, N. M.; Pandis, S. N. High Formation of Secondary Organic Aerosol from the Photo-Oxidation of Toluene. *Atmos. Chem. Phys.* **2009**, *9*, 2973−2986.
(90) Lopez-Hilfiker, F. D.; Mohr, C.; Ehn, M.; Rubach, F.; Kleist, E.; Wildt, J.; Mentel, T. F.; Lutz, A.; Hallquist, M.; Worsnop, D.; Thornton, J. A. A Novel Method for Online Analysis of Gas and Particle Composition: Description and Evaluation of a Filter Inlet for Gases and AEROsols (FIGAERO). *Atmos. Meas. Tech.* **2014**, *7*, 983−1001.
(91) Lopez-Hilfiker, F. D.; Mohr, C.; D'Ambro, E. L.; Lutz, A.; Riedel, T. P.; Gaston, C. J.; Iyer, S.; Zhang, Z.; Gold, A.; Surratt, J. D.; Lee, B. H.; Kurten, T.; Hu, W. W.; Jimenez, J.; Hallquist, M.; Thornton, J. A. Molecular Composition and Volatility of Organic Aerosol in the Southeastern U.S.: Implications for IEPOX Derived SOA. *Environ. Sci. Technol.* **2016**, *50*, 2200−2209.
(92) Liu, S.; Thompson, S. L.; Stark, H.; Ziemann, P. J.; Jimenez, J. L. Gas-Phase Carboxylic Acids in a University Classroom: Abundance, Variability, and Sources. *Environ. Sci. Technol.* **2017**, *51*, 5454−5463.
(93) Cui, T.; Zeng, Z.; dos Santos, E. O.; Zhang, Z.; Chen, Y.; Zhang, Y.; Rose, C. A.; Budisulistiorini, S. H.; Collins, L. B.; Bodnar, W. M.; de Souza, R. A. F.; Martin, S. T.; Machado, C. M. D.; Turpin, B. J.; Gold, A.; Ault, A. P.; Surratt, J. D. Development of a Hydrophilic Interaction Liquid Chromatography (HILIC) Method for the Chemical Characterization of Water-Soluble Isoprene Epoxydiol (IEPOX)-Derived Secondary Organic Aerosol. *Environ. Sci.: Process. Impacts* **2018**, *20*, 1524−1536.
(94) Aljawhary, D.; Lee, A. K. Y.; Abbatt, J. P. D. High-Resolution Chemical Ionization Mass Spectrometry (ToF-CIMS): Application to Study SOA Composition and Processing. *Atmos. Meas. Tech.* **2013**, *6*, 3211−3224.
(95) Lee, B. H.; Lopez-hil, F. D.; Mohr, C.; Kurte, T.; Worsnop, D. R.; Thornton, J. A. An Iodide-Adduct High-Resolution Time-of-Flight Chemical- Ionization Mass Spectrometer: Application to Atmospheric Inorganic and Organic Compounds. *Environ. Sci. Technol.* **2014**, 6309.
(96) Riva, M.; Rantala, P.; Krechmer, E. J.; Peräkylä, O.; Zhang, Y.; Heikkinen, L.; Garmash, O.; Yan, C.; Kulmala, M.; Worsnop, D.; Ehn, M. Evaluating the Performance of Five Different Chemical Ionization Techniques for Detecting Gaseous Oxygenated Organic Species. *Atmos. Meas. Tech.* **2019**, *12*, 2403−2421.
(97) Clegg, S. L.; Pitzer, K. S.; Brimblecombe, P. Thermodynamics of Multicomponent, Miscible, Ionic Solutions. Mixtures Including Unsymmetrical Electrolytes. *J. Phys. Chem. A* **1992**, *96*, 9470−9479.
(98) Wexler, A. S.; Clegg, S. L. Atmospheric Aerosol Models for Systems Including the Ions H +, NH 4 +, Na +, SO 4 2−, NO 3 −, Cl −, Br −, and H 2 O. *J. Geophys. Res.* **2002**, *107*, ACH 14-1.
(99) Nestorowicz, K.; Jaoui, M.; Rudzinski, K. J.; Lewandowski, M.; Kleindienst, T. E.; Spólnik, G.; Danikiewicz, W.; Danikiewicz, W.; Szmigielski, R. Chemical Composition of Isoprene SOA under Acidic and Non-Acidic Conditions: Effect of Relative Humidity. *Atmos. Chem. Phys.* **2018**, *18*, 18101−18121.
(100) Huang, Y.; Zhao, R.; Charan, S. M.; Kenseth, C. M.; Zhang, X.; Seinfeld, J. H. Unified Theory of Vapor-Wall Mass Transport in Teflon-Walled Environmental Chambers. *Environ. Sci. Technol.* **2018**, *52*, 2134.
(101) Budisulistiorini, S. H.; Canagaratna, M. R.; Croteau, P. L.; Marth, W. J.; Baumann, K.; Edgerton, E. S.; Shaw, S. L.; Knipping, E. M.; Worsnop, D. R.; Jayne, J. T.; Gold, A.; Surratt, J. D. Real-Time Continuous Characterization of Secondary Organic Aerosol Derived from Isoprene Epoxydiols in Downtown Atlanta, Georgia, Using the Aerodyne Aerosol Chemical Speciation Monitor. *Environ. Sci. Technol.* **2013**, *47*, 5686−5694.
(102) Finlayson-Pitts, B. J.; Keoshian, C. J.; Buehler, B.; Ezell, A. A. Kinetics of Reaction of Chlorine Atoms with Some Biogenic Organics. *Int. J. Chem. Kinet.* **1999**, *31*, 491−499.
(103) Cabañas, B.; Villanueva, F.; Salgado, M. S.; Martín, P.; Monedero, E.; Tapia, A. An Overview of the Atmospheric Reactions between Chlorine Atoms and Some Heterocyclic Compounds. *Trends Heterocycl. Chem.* **2011**, *15*, 1−22.
(104) Wang, W.; Kourtchev, I.; Graham, B.; Cafmeyer, J.; Maenhaut, W.; Claeys, M. Characterization of Oxygenated Derivatives of Isoprene Related to 2-Methyltetrols in Amazonian Aerosols Using Trimethylsilylation and Gas Chromatography/Ion Trap Mass Spectrometry. *Rapid Commun. Mass Spectrom.* **2005**, *19*, 1343−1351.
(105) Surratt, J. D.; Murphy, S. M.; Kroll, J. H.; Ng, N. L.; Hildebrandt, L.; Sorooshian, A.; Szmigielski, R.; Vermeylen, R.; Maenhaut, W.; Claeys, M.; Flagan, R. C.; Seinfeld, J. H. Chemical Composition of Secondary Organic Aerosol Formed from the Photooxidation of Isoprene. *J. Phys. Chem. A* **2006**, *110*, 9665−9690.
(106) Iyer, S.; Lopez-Hilfiker, F.; Lee, B. H. H.; Thornton, J. A. A.; Kurtén, T. Modeling the Detection of Organic and Inorganic

https://doi.org/10.1021/acs.est.1c07048
Environ. Sci. Technol. 2022, 56, 9251−9264

Compounds Using Iodide-Based Chemical Ionization. *J. Phys. Chem. A* **2016**, *120*, 576−587.
(107) Lopez-Hilfiker, F. D.; Iyer, S.; Mohr, C.; Lee, B. H.; D'ambro, E. L.; Kurtén, T.; Thornton, J. A. Constraining the Sensitivity of Iodide Adduct Chemical Ionization Mass Spectrometry to Multifunctional Organic Molecules Using the Collision Limit and Thermodynamic Stability of Iodide Ion Adducts. *Atmos. Meas. Tech.* **2016**, *9*, 1505−1512.
(108) Bi, C.; Krechmer, J. E.; Frazier, G. O.; Xu, W.; Lambe, A. T.; Claflin, M. S.; Lerner, B. M.; Jayne, J. T.; Worsnop, D. R.; Canagaratna, M. R.; Isaacman-VanWertz, G. Coupling a Gas Chromatograph Simultaneously to a Flame Ionization Detector and Chemical Ionization Mass Spectrometer for Isomer-Resolved Measurements of Particle-Phase Organic Compounds. *Atmos. Meas. Tech.* **2021**, *14*, 3895−3907.
(109) Lin, Y. H.; Zhang, H.; Pye, H. O. T.; Zhang, Z.; Marth, W. J.; Park, S.; Arashiro, M.; Cui, T.; Budisulistiorini, S. H.; Sexton, K. G.; Vizuete, W.; Xie, Y.; Luecken, D. J.; Piletic, I. R.; Edney, E. O.; Bartolotti, L. J.; Gold, A.; Surratt, J. D. Epoxide as a Precursor to Secondary Organic Aerosol Formation from Isoprene Photooxidation in the Presence of Nitrogen Oxides. *Proc. Natl. Acad. Sci. U.S.A.* **2013**, *110*, 6718−6723.
(110) Kjaergaard, H. G.; Knap, H. C.; Ørnsø, K. B.; Jørgensen, S.; Crounse, J. D.; Paulot, F.; Wennberg, P. O. Atmospheric Fate of Methacrolein. 2. Formation of Lactone and Implications for Organic Aerosol Production. *J. Phys. Chem. A* **2012**, *116*, 5763−5768.
(111) Edney, E. O.; Kleindienst, T. E.; Jaoui, M.; Lewandowski, M.; Offenberg, J. H.; Wang, W.; Claeys, M. Formation of 2-Methyl Tetrols and 2-Methylglyceric Acid in Secondary Organic Aerosol from Laboratory Irradiated Isoprene/NOX/SO 2/Air Mixtures and Their Detection in Ambient PM2.5 Samples Collected in the Eastern United States. *Atmos. Environ.* **2005**, *39*, 5281−5289.
(112) Claeys, M.; Graham, B.; Vas, G.; et al. Formation of Secondary Organic Aerosols Through Photooxidation of Isoprene. *Science* **2004**, *303*, 1173−1176.
(113) Jaoui, M.; Szmigielski, R.; Nestorowicz, K.; Kolodziejczyk, A.; Sarang, K.; Rudzinski, K. J.; Konopka, A.; Bulska, E.; Lewandowski, M.; Kleindienst, T. E. Organic Hydroxy Acids as Highly Oxygenated Molecular (HOM) Tracers for Aged Isoprene Aerosol. *Environ. Sci. Technol.* **2019**, 14516.
(114) Ezell, M. J.; Wang, W.; Ezell, A. A.; Soskin, G.; Finlayson-Pitts, B. J. Kinetics of Reactions of Chlorine Atoms with a Series of Alkenes at 1 Atm and 298 k: Structure and Reactivity. *Phys. Chem. Chem. Phys.* **2002**, *4*, 5813−5820.
(115) Wang, L.; Arey, J.; Atkinson, R. Reactions of Chlorine Atoms with a Series of Aromatic Hydrocarbons. *Environ. Sci. Technol.* **2005**, *39*, 5302−5310.

https://doi.org/10.1021/acs.est.1c07048
Environ. Sci. Technol. 2022, 56, 9251−9264